Alma Mater Studiorum · Università di Bologna

SCUOLA DI SCIENZE

Corso di Laurea in Matematica

Knotoids

Tesi di Laurea in Topologia

Relatore:
Prof.ssa
ALESSIA CATTABRIGA

Presentata da:
ALESSANDRO BONZI

Sessione autunnale
Anno Accademico 2019/2020

Alla mia famiglia.

Contents

Introduction

English

The aim of this thesis is to study the theory of knotoids. In particular, we will find some useful results that link it to knots and we will use these last outcomes to develop some techniques that allow us to study proteins.

The theory of knotoids is recent: it was introduced by Vladimir Turaev in 2012 as a ramification of that of knots. Intuively, knotoids can be seen as open knot diagrams, that is open curves embedded in a surface with the data of finitely many crossings. In particular, they were initially thought as knots missing a piece of their body. But there is another interesting way to relate knots to knotoids. Indeed, it is possible to use the theory of branched coverings to define a new connection between these two objects. Another aspect, the classification of knotoids still remains an open topic in the theory, even if some recent studies has achieved some great results in this field. Other researches have focused on determining how knotoids can be transformed into each other - due to their openness - and in studying these relations in order to classify knotoids basing on those. One of the most promising application of knotoids deals with proteins. Indeed, there is a tight connection between a specific function of a protein and the entanglement that it assumes. In this context, it has become more and more important to identify valid strategies for detecting how a protein change its structure in the space, and knotoids have been found to represent a privileged tool for doing this.

This work is divided into three chapters. The first one includes a recall

on knot theory, the presentation of knotoids, the description of an invariant of knotoids and the definition of θ-curves. The second chapter is dedicated to the formulation of the main results of this thesis. We will see how is it possible to move from knotoids to θ-curves and from θ-curves to strongly invertible knots, and what are the correspondences between these three objects. We will then see what are the consequences of applying a forbidden move on a knotoid k on its associated θ-curve and strongly invertible knot and we will show how is it possible to build a table of the f-distances between any two knotoids with up to four crossings. In the third and last chapter we will analyse some recent applications of the theory of knotoids to proteins. After having explained what is the connection between proteins and knotoids we will give an estimate of a good sample size for the number of projections needed to obtain a realistic and computationally feasible representation of the protein. Last, but not least, we will study the case of deeply knotted proteins, in particular finding a good and easy to calculate coefficient that encodes this useful information. At the end of this work there is an appendix that contains a table of knotoids with up to four crossings and a table of knots with up to eight crossings, in order to help the reader in understanding the knotoids and knots that are used throughout this work.

Italiano

L'obiettivo di questa tesi è di studiare la teoria dei nodoidi. In particolare, troveremo alcuni interessanti risultati che collegano questa teoria con quella dei nodi e useremo questi risultati ottenuti per sviluppare alcune tecniche volte allo studio delle proteine.

La teoria dei nodoidi è recente: è stata introdotta da Vladimir Turaev nel 2012 come ramificazione della teoria dei nodi. Intuitivamente, i nodoidi possono essere visti come diagrammi aperti di nodi, cioè curve aperte su una superficie con un'informazione sugli incroci (che devono essere un numero finito). In particolare, i nodoidi sono stati pensati come nodi in cui una

parte del corpo è stata rimossa. C'è però anche un altro modo interessante per mettere in relazione nodi e nodoidi. Infatti, è possibile usare la teoria dei rivestimenti ramificati per ottenere un nuovo legame fra i due. Inoltre, la classificazione dei nodoidi rimane tutt'ora un problema aperto della teoria, nonostante alcuni studi recenti abbiano fatto diversi passi avanti in questo senso. Altri ricercatori si sono invece concentrati sul modo in cui i nodoidi possono essere trasformati l'uno nell'altro - sfruttando il fatto che siano curve aperte - e su come classificare i nodoidi basandosi su queste relazioni. Altro aspetto interessante sono le applicazioni di questa teoria: una delle più promettenti riguarda le proteine. C'è infatti una stretta connessione tra alcune funzioni specifiche delle proteine e il loro modo di annodarsi. In questo ambito, sta assumendo sempre più rilevanza l'identificazione delle strategie migliori per riconoscere come le proteine cambiano la loro struttura nello spazio, e i nodoidi rappresentano valido strumento a riguardo.

Questo elaborato è diviso in tre capitoli. Il primo comprende un richiamo di teoria dei nodi, la presentazione dei nodoidi, l'introduzione di un invariante per nodoidi e la definizione delle θ-curve. Il secondo è dedicato alla formulazioni dei risultati principali di questa tesi. Vedremo come è possibile passare da nodoidi a θ-curve e da θ-curve a nodi fortemente invertibili, e quali sono le corrispondenze tra questi oggetti. Vedremo poi quali sono le conseguenze dell'applicazione di una mossa proibita su un nodoide sui rispettivi θ-curva e nodo fortemente invertibile e mostreremo come sia possibile costruire una tabulazione delle f-distances per nodoidi con numero minimo di incroci fino a quattro. Nel terzo e ultimo capitolo analizzeremo alcune delle recenti applicazioni della teoria dei nodoidi alle proteine. Dopo aver spiegato qual è il legame tra proteine e nodoidi daremo una stima per scegliere in maniera efficace la cardinalità del campione di dati esaminato, in modo da ottenere una rappresentazione della proteina che sia allo stesso tempo realistica e computazionalmente sostenibile. In ultimo, studieremo il caso di proteine "profondamente annodate" e in particolare definiremo l'area relativa, una buona indicazione numerica che ci aiuti a distinguere le pro-

teine profondamente annodate dalle altre. Alla fine dell'elaborato si trova una appendice che contiene una tabella di identificazione dei nodoidi fino a quattro incroci e una dei nodi fino a otto incroci, per aiutare il lettore nel visualizzare i nodi e nodoidi che vengono usati in questa tesi.

Chapter 1

Basic definitions

The theory of knotoids naturally arises as a generalisation of that of knots. In this chapter we firstly do a recall on the basics of this theory (following [3]), as we will need some of its main concepts thoughout this thesis. Secondly, we introduce knotoids in Section 1.2. In Section 1.3 we analyse an important invariant of knotoids, the extended bracket polynomial (following [8]), that can be used to create a table of knotoids (that can be found in Appendix A). Section 1.4 is committed to the description of another object that will be crucial in our study of knotoids: the θ-curves. The concepts of Section 1.2 and 1.4 are taken from [1, Sections from 1 to 3] unless it is differently specified.

1.1 Recall on knot theory

Definition 1.1. *A **tame knot** is a PL or smooth embedding of S^1 in the Euclidean space (or in the 3-sphere S^3 with the Euclidean metric) considered up to ambient isotopies*

where

Definition 1.2. *Two embeddings $f_0, f_1 : X \longrightarrow Y$ are **ambient isotopic** if there is a level preserving PL or smooth isotopy*

$$H : Y \times I \longrightarrow Y \times I, \quad H(y,t) = (h_t(y), t)$$

where $h_0 = id_Y$ and $f_1 = h_1 f_0$. The mapping H is called ***ambient isotopy****.*

We will refer to tame knots just as **knots**. Let us call $\mathcal{K}(S^3)$ the set of oriented knots in the 3-dimensional sphere: a knot is **oriented** if it is given together with the data of an orientation, a chosen direction to travel around the knot (in figures it is represented by an arrow on the knot).

Given a knot we can project it onto a plane. We require that the projection has a finite number of multiple points that must be at most double points; moreover, it must not have cusps or tangent lines. If at any double point of the projection we give the data of over/under-crossing we obtain what we call a **knot diagram**. The concept of equivance of knots extends to knot diagrams:

Definition 1.3. *Two knot diagrams are said to be* ***equivalent*** *if they are connected by a finite sequence of ambient isotopies of diagrams that preserve the data of over/under crossings and of* ***Reidemeister moves*** *Ω_i, $i = 1, 2, 3$. The moves are described in Figure 1.1.*

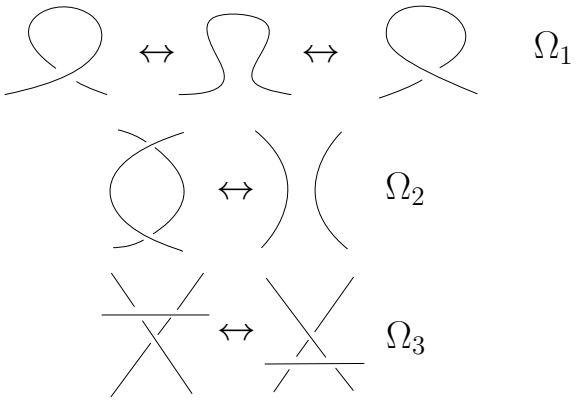

Figure 1.1: The classical Reidemeister moves Ω_1, Ω_2 and Ω_3.

Note that Reidemeister moves consist in a local change in the diagram of a knot. Moreover

Theorem 1.1. *Two knots are equivalent if and only if all their diagrams are equivalent.*

We are not interested just in knots, but in what we call strongly invertible knots:

Definition 1.4. *A **strongly invertible knot** is the pair (K, τ) where $K \in \mathcal{K}(S^3)$ and $\tau \in Sym^+(S^3, K)$ is an involution of S^3 called **strong inversion** that reverses the orientation of K, taken up to conjugacy in $Sym^+(S^3, K)$. Thus, two strongly invertible knots (K_1, τ_1) and (K_2, τ_2) are **equivalent** if there is an orientation preserving homeomorphism $f : S^3 \longrightarrow S^3$ satifying $f(K_1) = K_2$ and $f\tau_1 f^{-1} = \tau_2$.*

Let us call $\mathcal{KSI}(S^3)$ the set of strongly invertible knots (K, τ) in S^3 and $\mathcal{K}_{\mathcal{S}.\mathcal{I}.}(S^3)$ the subset of $\mathcal{K}(S^3)$ of knots that admit a strong inversion. The set of fixed points of a strong inversion τ will be denoted with $\mathrm{Fix}(\tau)$.

1.2 Knotoids

There are two possible definitions of knotoids: we can see them as immersed arcs in $\mathbb{R}^2$ or in the sphere S^2. In both cases knotoids have the same properties and there is a surjective but non injective map from the knotoids in $\mathbb{R}^2$ to those in S^2 (see Figure 1.2). As the theory we want to develop is exhaustive in S^2 and due to the aim of this thesis we will not deal with knotoids in $\mathbb{R}^2$ (for more information see [1]). As for knots, we can give the definition of a knotoid diagram and of equivalence between these diagrams.

Definition 1.5. *A **knotoid diagram** in S^2 is a generic immersion of the interval $[0, 1]$ in S^2 with finitely many transverse double points endowed with over/under-crossing data. The images of the **endpoints** 0 and 1, called v_0 the **tail** and v_1 the **head** of the knotoid diagram, are distinct from any other point and from each other. We consider knotoids as oriented from the tail to the head (see Figure 1.2).*

Definition 1.6. *A **knotoid** is an equivalence class of knotoid diagrams on the sphere up to ambient isotopies of S^2, respecting the under/over crossing*

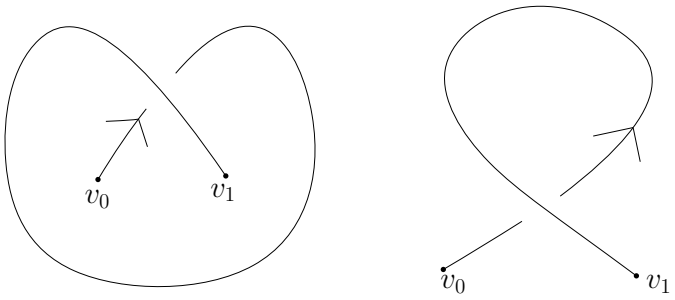

Figure 1.2: The diagrams in the picture represent oriented knotoids that are different if seen in $\mathbb{R}^2$, but that are the same if considered as knotoids in S^2.

data, and the three classical Reidemeister moves performed away from the endpoints.

It is not permitted to pull the strand adjacent to an endpoint over/under a transversal strand (as shown in Figure 1.3). Indeed, allowing these moves, that are called **forbidden moves**, produces a trivial theory (for a more precise definition see Definition 2.3).

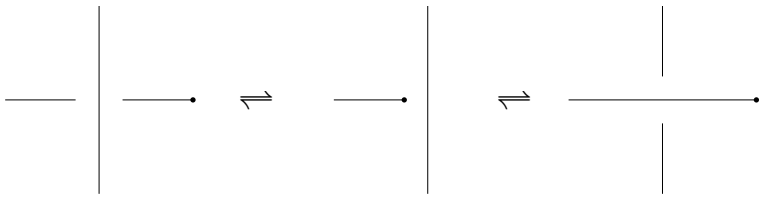

Figure 1.3: Forbidden Moves.

Let us denote by $\mathbb{K}(S^2)$ the set of oriented knotoids in the sphere. We can give this set an operation of multiplication defined as follows. First, note that each endpoint of a knotoid k in S^2 admits a neighbourhood D such that k intersects it in just one arc (a radius) of D. Such a neighbourhood is called a **regular neighbourhood** of the endpoint. Given two diagrams in S^2 representing the knotoids k_1 and k_2 equipped with a regular neighbourhood D_1 for the head of k_1 and D_2 for the tail of k_2, the **product knotoid** $k = k_1 \cdot k_2$ is defined as the equivalence class in $\mathbb{K}(S^2)$ of the diagram obtained by gluing $S^2 \setminus \mathrm{Int}(D_1)$ to $S^2 \setminus \mathrm{Int}(D_2)$ through an orientation-reversing homeomorphism

$\partial D_1 \longrightarrow \partial D_2$ mapping the only point in $\partial D_1 \cap k_1$ to the only point in $\partial D_2 \cap k_2$ (see Figure 1.4). Note that this operation is not commutative and it turns $\mathbb{K}(S^2)$ into a semigroup.

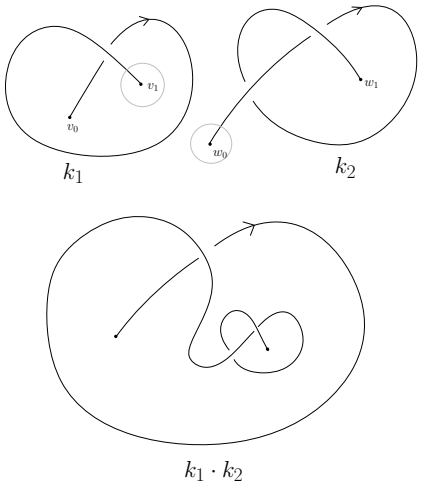

Figure 1.4: On the bottom line, a diagram representing the product $k_1 \cdot k_2$ of the knotoids in the upper line; the circles in grey are the regular neighbourhoods of the endpoints v_1 and w_0.

We can define four commuting involutions on knotoids in $\mathbb{K}(S^2)$ (see Figure 1.5). Given a knotoid k:

- its **reversion** (whose result is denoted with $-k$) consists in changing the orientation of the knotoid or, in other words, exchanging the labels of the endpoints;
- its **mirror reflection** tranforms k in the knotoid k_m with the same diagram but with all the crossings changed;
- its **symmetry** produces the knotoid $\mathrm{sym}(k)$ derived from the extension to S^2 of the reflection of $\mathbb{R}^2$ along the horizontal line passing through the endpoints of k;
- its **rotation** is defined as $k_{\mathrm{rot}} = (\mathrm{sym}(k))_m$.

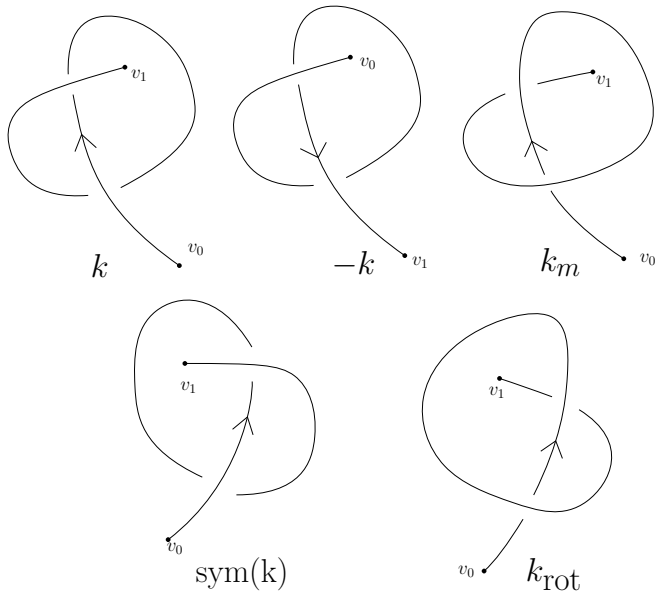

Figure 1.5: A knotoid k, its reverse $-k$, its mirror image k_m, its symmetric $\text{sym}(k)$ and its rotation k_{rot}.

To this end we introduce two more notations: let us call $\mathbb{K}(S^2)/_\sim$ the quotient of $\mathbb{K}(S^2)$ up to reversion and $\mathbb{K}(S^2)/_\approx$ the quotient of $\mathbb{K}(S^2)$ up to reversion and rotation.

1.3 Extended bracket polynomial of knotoids

We would like to produce a table of all knotoids in the sphere, that is, a list of all distinct knotoids in S^2. This is possible by means of some knotoids invariants, that is, some quantities that represent a necessary condition for the knotoids to be equivalent. In other words, two knotoids k and k' cannot be equivalent if an invariant associated to k is different to the one associated to k'. There are several examples of invariants: they can be numbers, polynomials or general characteristics of the object considered. In this section we will describe how to define a knotoid invariant called extended bracket polynomial, which in particular is a polynomial (following [8]).

1.3.1 Normalised bracket polynomial

Definition 1.7. *Let $k \subset S^2$ be a knotoid diagram. A **state** on K is a mapping from the set of crossings of k to the set $\{-1, 1\}$.*

Definition 1.8. *Given a knotoid $k \subset S^2$ and a state s we define **A-smoothings** and **B-smoothings** as below:*

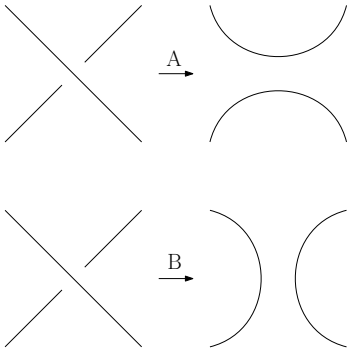

Figure 1.6: A-smoothing on the top and B-smoothing on the bottom.

Given a state s on k, we apply the A-smoothings (resp. B-smoothings) at all crossings of k with positive (resp. negative) value of s. This yelds to a compact 1-manifold $k_s \subset S^2$ consisting of a single embedded segment (that connects the endpoints) and several disjoint embedded circles. We define the Laurent polynomial

$$\langle k \rangle = \sum_{s \in S(k)} A^{\sigma_s}(-A^2 - A^{-2})^{|s|-1}$$

where $S(k)$ is the set of all states of k, $\sigma_s \in \mathbb{Z}$ is the sum of the values ± 1 of $s \in S(k)$ over all crossings of k and $|s|$ is the number of components of k_s. It is possible to show with standard computations that the Laurent polynomial $\langle k \rangle \in \mathbb{Z}[A^{\pm 1}]$ is invariant under the second and third Reidemeister moves and is multiplied by $(-A^3)^{\pm 1}$ under the first Reidemeister moves. Hence, the polynomial $\langle k \rangle$ considered up to multiplication by integral powers of $-A^3$ is an invariant of knotoids called the **bracket polynomial**.

Remark 1. One useful invariant of knotoids derived from the bracket polynomial is the span. Given a non-zero Laurent polynomial $f = \sum_i f_i A^i \in \mathbb{Z}[A^{\pm 1}]$ its **span** is defined by $\mathrm{spn}(f) = i_+ - i_-$ where i_+ (resp. i_-) is the maximal (resp. minimal) integer i such that $f_i \neq 0$. For $f = 0$ set $\mathrm{spn}(f) = -\infty$. The **span** of a knotoid k is defined as $\mathrm{spn}(k) = \mathrm{spn}(\langle k \rangle)$. Clearly $\mathrm{spn}(k)$ is invariant under all Reidemeister moves and defines a knotoid invariant also denoted with spn. It is always an even, non-negative integer.

We can solve the effect of the first Reidemeister moves on the bracket polynomial using the writhe.

Definition 1.9. *The* ***writhe*** $w(k) \in \mathbb{Z}$ *of a knotoid* k *is the sum of the signs of all the crossings of* k *following the rule below (recalling that a knotoid is oriented from the tail to the head):*

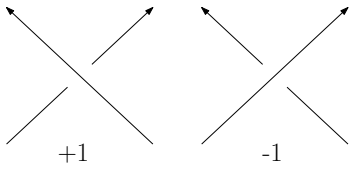

The product $\langle k \rangle_\circ = (-A^3)^{-w(k)} \langle k \rangle$ is invariant under all three Reidemeister moves and hence its associated function, called **normalised bracket polynomial**, is an invariant of knotoids.

Remark 2.

- The normalised bracket polynomial is invariant under reversion of knotoids and changes via $A \longmapsto A^{-1}$ under mirror reflection;
- the normalised bracket polynomial is multiplicative: we have that $\langle k_1 k_2 \rangle_\circ = \langle k_1 \rangle_\circ \langle k_2 \rangle_\circ$ for any knotoids k_1 and k_2 in S^2.

The next example (that concludes this section) shows how the normalised bracket polynomial can distinguish knotoids.

Example 1.1. Let us consider the knotoids 3_1 and 3_2 of Appendix A and let us calculate the normalised bracket polynomial for these knotoids. Figure 1.7 shows the smoothings k_s performed on the two knotoids, regarding

all their states, while Table 1.7 reports the values, for any state s, of σ_s and $|s|$ enumerated with respect to Figure 1.7 of the two knotoids. Drawings corresponding to the same state s share the same number.

Drawing number	$s = (R, S, T)$	σ_s	$\|s\|$ of 3_1	$\|s\|$ of 3_2
1	$(1, 1, 1)$	3	3	2
2	$(1, 1, -1)$	1	2	1
3	$(1, -1, 1)$	1	2	1
4	$(1, -1, -1)$	-1	1	1
5	$(-1, 1, 1)$	1	2	2
6	$(-1, 1, -1)$	-1	1	1
7	$(-1, -1, 1)$	-1	1	1
8	$(-1, -1, -1)$	-3	2	2

We now compute the two polynomials, noting that $w(3_1) = 3$ and $w(3_2) = 1$:

$$\begin{aligned}
\langle 3_1 \rangle_\circ &= (-A^3)^{-w(3_1)} \sum_{s \in S(3_1)} A^{\sigma_s} (-A^2 - A^{-2})^{|s|-1} = \\
&= (-A^3)^{-3} [A^3(-A^2 - A^{-2})^2 + 3A^1(-A^2 - A^{-2})^1 + 3A^{-1}(-A^2 - A^{-2})^0 + \\
&+ A^{-3}(-A^2 - A^{-2})^1] = \\
&= -A^{-9}[A^7 - A^3 - A^{-5}] = \\
&= -A^{-2} + A^{-6} + A^{-14}.
\end{aligned}$$

$$\begin{aligned}
\langle 3_2 \rangle_\circ &= (-A^3)^{-w(3_2)} \sum_{s \in S(3_2)} A^{\sigma_s} (-A^2 - A^{-2})^{|s|-1} = \\
&= (-A^3)^{-1} [A^3(-A^2 - A^{-2})^1 + 2A^1(-A^2 - A^{-2})^0 + 3A^{-1}(-A^2 - A^{-2})^0 + \\
&+ A^1(-A^2 - A^{-2})^1 + A^{-3}(-A^2 - A^{-2})^1] = \\
&= -A^{-3}[-A^5 - A^3 + A + A^{-1} - A^{-5}] = \\
&= A^2 + 1 - A^{-2} - A^{-4} + A^{-8}.
\end{aligned}$$

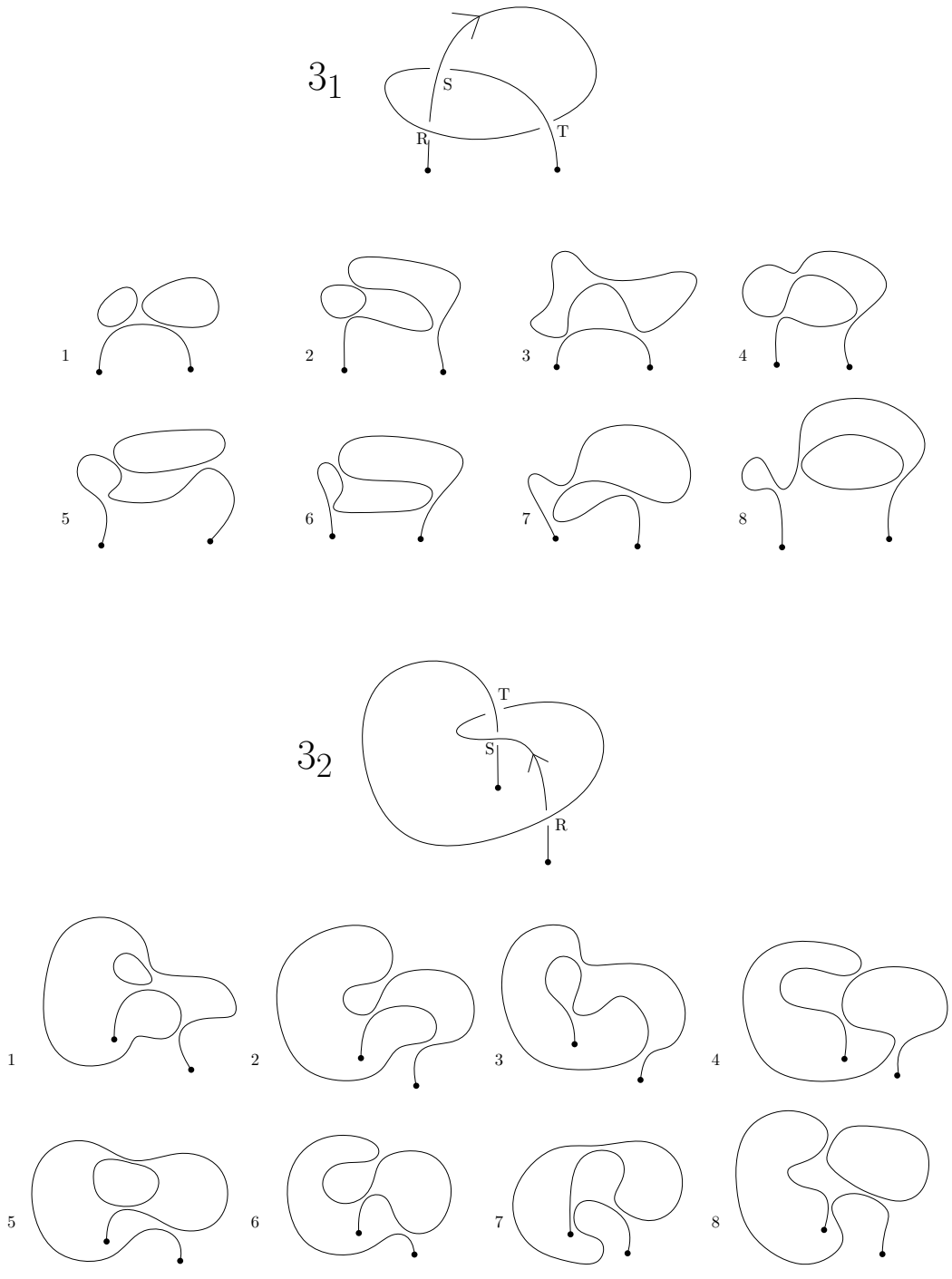

Figure 1.7: The two knotoids 3_1 and 3_2 and all their possible smoothings.

As these polynomials are different, the knotoids 3_1 and 3_2 are not equivalent.

1.3.2 Extended bracket polynomial

Let us now show how to proceed with the construction of the extended bracket polynomial of knotoids, which is a 2-variables extension of the normalised bracket polynomial of knotoids. Let us start with a preliminary definition:

Definition 1.10. *Given a knotoid $k \in \mathbb{K}(S^2)$, a* ***shortcut*** *$a \subset S^2$ for k is an embedded arc in S^2 connecting the endpoints of k and otherwise meeting k transversally at a finite number of points distinct from the crossings of k such that a passes everywhere under k.*

Let us consider a knotoid $k \in \mathbb{K}(S^2)$, and a shortcut a for k. Then, $k \cup a$ is a knot diagram. Given a state $s \in S(k)$ consider the smoothed 1-manifold k_s (a is not affected by the smoothings as they are applied in small neighbourhoods of the crossings of k) and its segment component j_s. As j_s coincides with k in a small neighbourhood of the endpoints of k, and the set $\partial j_s = \partial a$ consists of the endpoints of k, we can orient k, k_s and j_s from the tail to the head of k. Moreover, we denote with $j_s \cdot a$ the algebraic number of intersections of j_s with a, that is, the number of times that j_s crosses a from the right to the left minus the number of times that j_s crosses a from the left to the right (the endpoints of j_s and a are not counted). Similarly, we denote with $k \cdot a$ the algebraic number of intersections of k with a. We define a 2-variable Laurent polynomial $\langle\langle k \rangle\rangle_\circ \in \mathbb{Z}[A^{\pm 1}, u^{\pm 1}]$ by

$$\langle\langle k \rangle\rangle_\circ = (-A^3)^{-w(k)} u^{-k \cdot a} \sum_{s \in S(k)} A^{\sigma_s} u^{j_s \cdot a} (-A^2 - A^{-2})^{|s|-1}.$$

Lemma 1.2. *The polynomial $\langle\langle k \rangle\rangle_\circ$ does not depend on the the choice of the shortcut a and is invariant under the Reidemeister moves on k.*

Proof. Any two shortcuts for k are isotopic in the class of embedded arcs in S^2 connecting the endpoints of k. Therefore to verify the independence of a it is enough to analyse the following local transformations for a:

1. pulling a across a strand of k (this adds two points to $a \cap k$);

2. pulling a across a double point of k;

3. adding a curl to a near an endpoint of k (this adds one point to $a \cap k$).

The transformations (1) and (2) preserve the numbers $k \cdot a$ and $j_s \cdot a$ for all the states s of k. The transformation (3) preserves $j_s \cdot a - k \cdot a$ for all s. Hence $\langle\langle k \rangle\rangle_\circ$ is preserved under these transformations and does not depend on a.

Let us now verify that $\langle\langle \rangle\rangle_\circ$ is invariant under Reidemeister moves. Consider the unnormalised version $\langle\langle k, a \rangle\rangle$ of $\langle\langle k \rangle\rangle_\circ$ obtained by deleting the factor $(-A^3)^{-w(k)} u^{-k \cdot a}$. The polynomial $\langle\langle k, a \rangle\rangle$ depends on a but not on the orientation of k (to compute $j_s \cdot a$ it is important to know just which endopoint is the tail and which is the head of k). A standard argument on this polynomials shows that $\langle\langle k, a \rangle\rangle$ is invariant under the second and third Reidemeister moves and it is multiplied by $(-A^3)^{\pm 1}$ under the first Reidemeister moves (provided these moves are applied away from a). Such moves preserve the number $k \cdot a$ and therefore they preserve $\langle\langle k \rangle\rangle_\circ$. Since the polynomial does not depend on a, it is invariant under all Reidemeister moves on k. □

This lemma guarantees that the polynomial defined is actually an invariant of knotoids that will be called **extended bracket polynomial** and that will be denoted with $\langle\langle \rangle\rangle_\circ$.

As we said at the beginning of this section, knotoids invariants can be used to classify knotoids. In particular, in Appendix A it is possible to find a table (taken from [4]) of all distinct knotoids in the sphere with up to four crossings.

1.4 Theta-curves

In this section we introduce (following [1]) another interesting object, the θ-curves, that will be extremely useful in the development of this thesis.

Definition 1.11. *A **labelled θ-curve** is a graph embedded in S^3 with two vertices v_0 and v_1 (the **tail** and the **head** respectively) and three edges e_+, e_- and e_0 each of which joins v_0 to v_1. The curves $e_- \cup e_+$, $e_+ \cup e_0$ and $e_0 \cup e_-$ are called **constituent knots** of the θ-curve. A θ-curve is called **simple** if its constituent knot $e_- \cup e_+$ is the trivial knot. We will call two labelled θ-curves **isotopic** if they are related by an ambient isotopy that preserves the labels of the vertices and the edges (see Figure 1.8).*

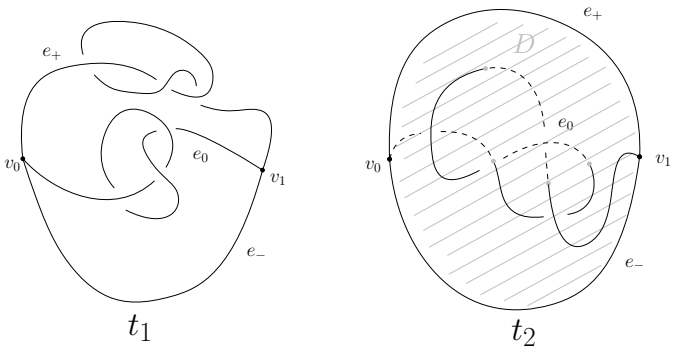

Figure 1.8: A non-simple θ-curve t_1 and a simple θ-curve t_2 with spanning disk D (the points in grey in the right part represent the intersection between the edge e_0 and the spanning disk D).

Let us call Θ^s the set of isotopy classes of simple labelled θ-curves. This set becomes a semigroup with an operation of vertex-multiplication defined in the following way (see [8]). Given θ-curves θ and θ', pick regular neighbourhoods B and B' of the head of θ and of the tail of θ', respectively. The vertex-multiplication $\theta \cdot \theta'$ of θ and θ' is given by the class of ambient isotopies of θ-curves of the diagram obtained by gluing the closed 3-balls $S^3 \backslash \mathrm{Int}(B)$ and $S^3 \backslash \mathrm{Int}(B')$ through an orientation reversing homeomorphism $\partial B \longrightarrow \partial B'$ carrying the only point of ∂B lying on the i-th edge of θ to the

only point of $\partial B'$ lying on the i-th edge of θ' for $i = +, 0, -$. This operation is associative.

To conclude this section (and this chapter) let us give a further definition:

Definition 1.12. *For a simple θ-curve θ there is an embedded 2-disk $D \subset S^3$ such that ∂D is the preferred constituent knot of the θ-curve. Deforming slightly D in S^3 keeping ∂D we may assume that $\mathrm{Int}(D)$ meets e_0 transversely at a finite number of points. We call such D a* ***spanning disk*** *for θ (see Figure 1.8).*

Chapter 2

The theory of Knotoids

In this chapter we deal with the main theorems that concern the theory of knotoids. In Section 2.1 we see how it is possibe to move from knotoid to θ-curves and what is the correspondence determined in this way (following [8]). In Section 2.2 we then relate θ-curves with strongly invertible knots, and from this we derive an important result on the correspondence between knotoids and strongly invertible knots (following [1]). In Section 2.3 we investigate the effects of a forbidden move (applied to a knotoid) on its correspondent θ-curve and strongly invertible knot (following [2]). In Section 2.4 we make a further step in the study of forbidden moves of knotoids; in particular, we describe (following [2]) how it is possible to build a table of the forbidden moves-distances between all the knotoids with up to four crossings.

2.1 Knotoids and theta-curves

Let us show how knotoids can be related with θ-curves (following [1]). Consider a knotoid diagram k in S^2. We can identify the sphere in which the diagram is immersed with $S^2 \times \{0\} \subseteq S^2 \times [-1, 1]$. We can embed k in $S^2 \times [-1, 1]$ by pushing the overpasses of the diagram into $S^2 \times [0, 1]$ and the underpasses into $S^2 \times [-1, 0]$ (see Figure 2.1). In particular, thw wndpoints v_0 and v_1 of the knotoid can be moved, but as far as they remain on two

preferred lines that are orthogonal to $S^2 \times \{0\}$. If we collapse $S^2 \times \partial I$ to two points, k becomes an embedded curve in S^3 with endpoints lying on an unknotted circle, as in Figure 2.2.

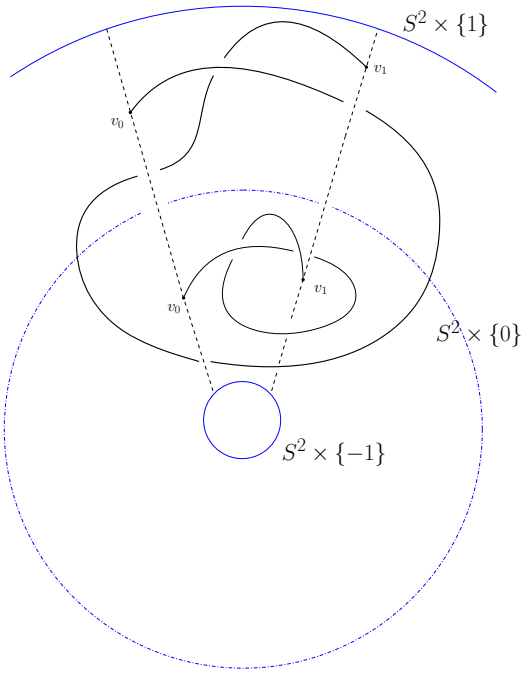

Figure 2.1: The thicker curve is the image in $S^2 \times [-1, 1]$ of the knotoid diagram in $S^2 \times \{0\}$ in the middle of the figure after having pushed the overpasses/underpasses in the upper-half/lower-half respectivley. Note that the endpoints v_0 and v_1 lie on two preferred lines, black and dashed in figure, that ensure that the knot type remains unchanged.

Thus, we can associate a simple labelled θ-curve to a knotoid $k \in \mathbb{K}(S^2)$ with vertices the endpoints of k and edge $e_0 = k$. We label the remaining edges of the curve in this way: the edge containing the image of $S^2 \times \{1\}$ under the collapsing map is labelled e_+, while the one containing the image of $S^2 \times \{-1\}$ is labelled e_-. The unknotted circle $e_- \cup e_+$ will be called the **preferred constituent unknot** of the θ-curve; it will always be represented as a dashed circle in figures, see the right part of Figure 2.2 for an example.

It is shown in [8] that the construction above induces a well defined map t between the semigroups $\mathbb{K}(S^2)$ and Θ^s. Moreover

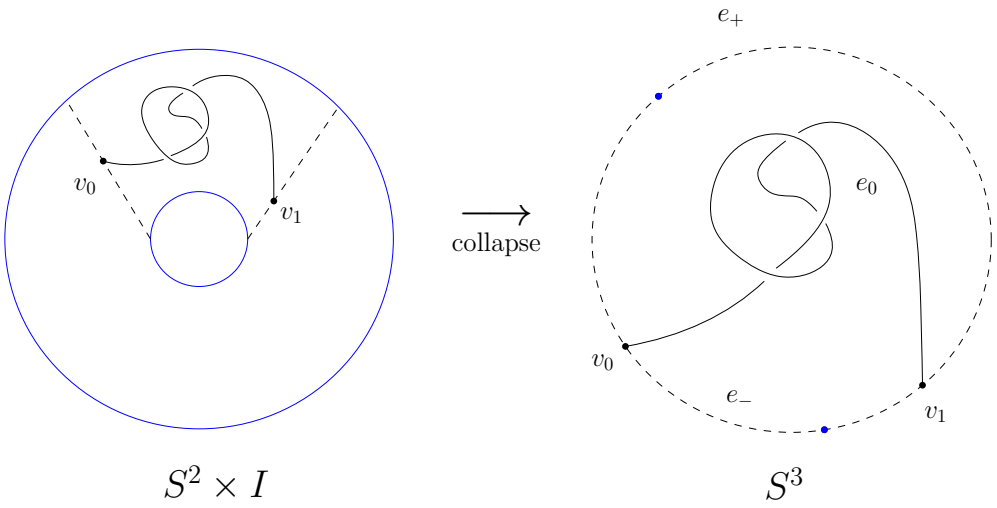

Figure 2.2: On the left, a knotoid seen as an embedded curve in $S^2 \times I$ with endpoints lying on the dashed lines. By collapsing $S^2 \times \partial I$ (in blue) to the two blue points on the right we obtain an embedded arc in S^3, with endpoints lying on a dashed circle (the image of the dashed lines). The dashes are just a graphic tool to visualise the preferred constituent unknot; it will remain so for the whole thesis.

Theorem 2.1. *The map $t : \mathbb{K}(S^2) \longrightarrow \Theta^s$ is a semigroup isomorphism.*

In order to prove this theorem we need a geometric lemma that we shall not prove:

Lemma 2.2 (Lemma 6.1 in [8])**.** *An orientation preserving diffeomorphism $f : S^3 \longrightarrow S^3$ fixing pointwise an unknotted circle $S \subset S^3$ is isotopic to the identity* $\mathrm{id} : S^3 \longrightarrow S^3$ *in the class of diffeomorphisms $S^3 \longrightarrow S^3$ fixing S pointwise.*

Proof. (of Theorem 2.1) That t transforms multiplication of knotoids into vertex-multiplication of θ-curves is clear from definitions. To prove that t is bijective we construct the inverse map $\Theta^s \longrightarrow \mathbb{K}(S^2)$.

Let $\theta \subset S^3 = \mathbb{R}^3 \cup \{\infty\}$ be a θ-curve with vertices v_0 and v_1 and edges e_-, e_0, e_+. We say that θ is **standard** if $\theta \subset \mathbb{R}^3$, both vertices lie in $\mathbb{R}^2 = \mathbb{R}^2 \times \{0\}$, e_+ lies in the upper half-space, e_- lies in the lower half-space and both e_- and e_+ projet bijectively to the same arc $a \subset \mathbb{R}^2$ connecting v_0 and

v_1. A standard θ-curve has a "standard" spanning disk D bounded by $e_- \cup e_+$ in $a \times \mathbb{R}$.

Observe that any simple θ-curve $\theta \subset S^3$ is ambient isotopic to a standard θ-curve (isotoping it away from ∞ and putting it in a standard position as above).

As we want to work with just standard θ-curves we need to show that if two standard θ-curves $\theta_1, \theta_2 \in \mathbb{R}^3$ are isotopic, then they are isotopic in the class of standard θ-curves. Indeed, we can easily deform θ_2 in the class of standard θ-curves so that θ_1 and θ_2 share the same vertices and the same $\pm$-labelled edges. Let S be the union of these vertices and edges, which is an unknotted circle in S^3. Since θ_1 is isotopic to θ_2 there is an orientation-preserving diffeomorphism $f : S^3 \to S^3$ carrying θ_1 to θ_2 and preserving the labels of the vertices and edges. Then $f(S) = S$. Deforming f we can additionally assume that $f_{|_S} = \mathrm{id}$. By Lemma 2.2, f is isotopic to the identity $\mathrm{id} : S^3 \to S^3$ in the class of diffeomorphisms fixing S pointwise. This isotopy induces an isotopy of θ_2 to θ_1 in the class of standard θ-curves.

The results above show that without loss of generality we can focus on the class of standard θ-curves and their isotopies in this class. Consider a standard θ-curve $\theta \subset \mathbb{R}^3$. We shall apply to θ a sequence of ambient isotopies that move the interior of e_0 and keep fixed the other edges and vertices. Let us call the standard spanning disk $D \subset a \times \mathbb{R}$ of θ as above. First, we isotope e_0 such that it meets $a \times \mathbb{R}$ transversely in a finite number of points. The intersections of e_0 with $a \times \mathbb{R} \setminus D$ can be eliminated by pulling the corresponding branches of e_0 horizontally across $v_0 \times \mathbb{R}$ or $v_1 \times \mathbb{R}$. In this way we can isotope e_0 so that all the intersections with $a \times \mathbb{R}$ lie inside D. Then we further isotope e_0 so that its projection onto $\mathbb{R} \times \{0\}$ has only double transversal crossings. This projection is provided with the data of over/under-crossings in the usual way and it becomes a knotoid diagram. The knotoid $u(\theta) \in \mathbb{K}(S^2)$ that corresponds to this diagram depends on θ only and it does not depend on the choices made in the construction. The key point is that pulling a branch across $v_0 \times \mathbb{R}$ or $v_1 \times \mathbb{R}$ lead to equivalent

knotoids in S^2. All the other isotopies are translated to sequences of isotopies or Reidemeister moves on the knotoid diagram away from the endpoints. Observe finally that the knotoid $u(\theta)$ is preserved under isotopy of θ in the class of standard θ-curves. Therefore u is a well-defined map $\Theta^s \to \mathbb{K}(S^2)$. It is clear that the maps t and u are mutually inverse. □

Let us now consider how the θ-curves vary under the involutions of Section 1.2. It should be clear that the θ-curves associated to a knotoid and its reverse differ by exchanging the labels of the vertices. Consider now a knotoid k and its rotation k_{rot}. It should be easy to see that their corresponding θ-curves differ from each other by simply swapping the labels of the edges e_+ and e_- and leaving all the other labels unchanged (see Figure 2.3). Calling $\Theta^s/_\sim$ the set of simple θ-curves up to relabelling the two vertices, the isomorphism t of Theorem 2.1 gives a bijection

$$t_\sim : \mathbb{K}(S^2)/_\sim \longrightarrow \Theta^s/_\sim$$

Furthermore, t also induces a bijection

$$t_\approx : \mathbb{K}(S^2)/_\approx \longrightarrow \Theta^s/_\approx$$

from the set of unoriented knotoids up to rotation and the set of simple θ-curves up to relabelling the vertices and the edges.

2.2 Knotoids and strongly invertible knots

What we want to do is to show how to define a construction that allows us to move from knotoids to knots (in particular to strongly invertible knots) and vice-versa. This will be possible by means of a double branched covering.

2.2.1 Double branched coverings

Let us give some of the main concepts of the theory of branched coverings before analysing how to construct it in our case (see [6, Section 22]).

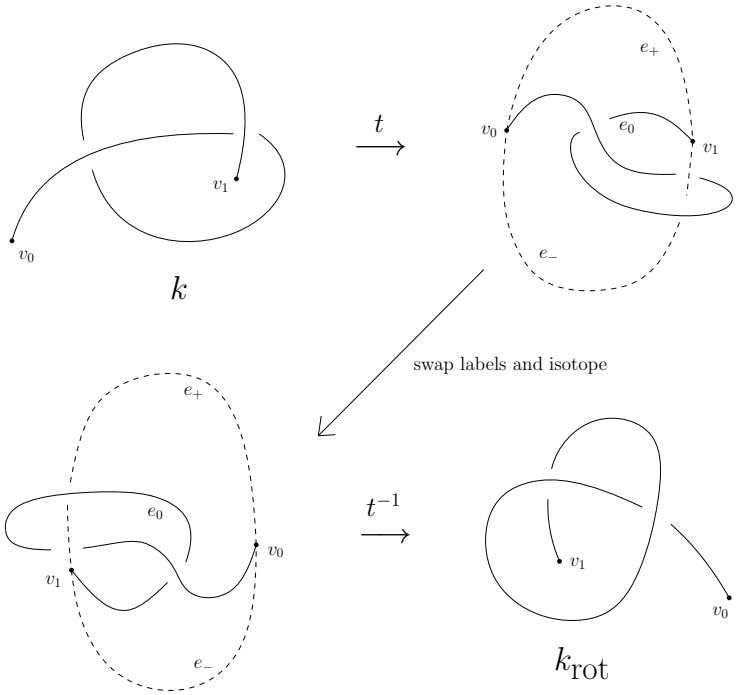

Figure 2.3: A knotoid and its rotation are associated to θ-curves differing from each other by swapping the e_- and e_+ labels.

Definition 2.1. *A **branched covering** of 3-manifolds M^3 and N^3 is a map $p : M^3 \longrightarrow N^3$ such that there exists one-dimensional subcomplex L^1 of N^3 whose inverse image $p^{-1}(L^1)$ is a one-dimensional subcomplex such that the restriction of p on its complement $M^3 \setminus p^{-1}(L^1)$ is a covering. M^3 is called the **covering set**, N^3 the **base** and L^1 the **branching set**. If $n \in \mathbb{N}$ is the cardinality of the fiber (the pre-image) of any point of $N^3 \setminus L^1$ the covering is said to be an **n-fold** covering. If $n = 2$ we call the branched covering a **double branched covering**.*

Definition 2.2. *A branched covering $p : M^3 \longrightarrow N^3$ is called **cyclic** if the group of the automorphisms of the covering obtained restricting p to $M^3 \setminus p^{-1}(L^1)$ is cyclic.*

In our case both M^3 and N^3 are S^3. In particular, we can construct a cyclic branched covering of S^3 branching on the unknot in the following way. Consider $S^3 = \mathbb{R}^3 \cup \infty$, choose a straight line $l \subseteq \mathbb{R}^3$ and, for some $n \in \mathbb{N}$,

consider G_n the group of the rotations by angle $2\pi\frac{k}{n}$ around the line l. It is easy to see that the action of G_n on $\mathbb{R}^3 \setminus l$ is properly discontinuous, so the natural projection $p_1' : \mathbb{R}^3 \setminus l \longrightarrow (\mathbb{R}^3 \setminus l)/G_n$ is a regular n-fold covering of $\mathbb{R}^3 \setminus l$. As $\mathbb{R}^3/G_n \cong \mathbb{R}^3$ we can write $p_1' : \mathbb{R}^3 \setminus l \longrightarrow \mathbb{R}^3 \setminus l$ and its extension $p_1 : \mathbb{R}^3 \longrightarrow \mathbb{R}^3$ to $\mathbb{R}^3$ is a branched covering of $\mathbb{R}^3$ with branching set l. The further extension $p : S^3 \longrightarrow S^3$ of this map to $S^3 = \mathbb{R}^3 \cup \infty$ results in a cyclic branched covering with branching set the circle $l \cup \infty$. Moreover, $l \cup \infty$ is also the inverse image of the branching set (see Figure 2.4).

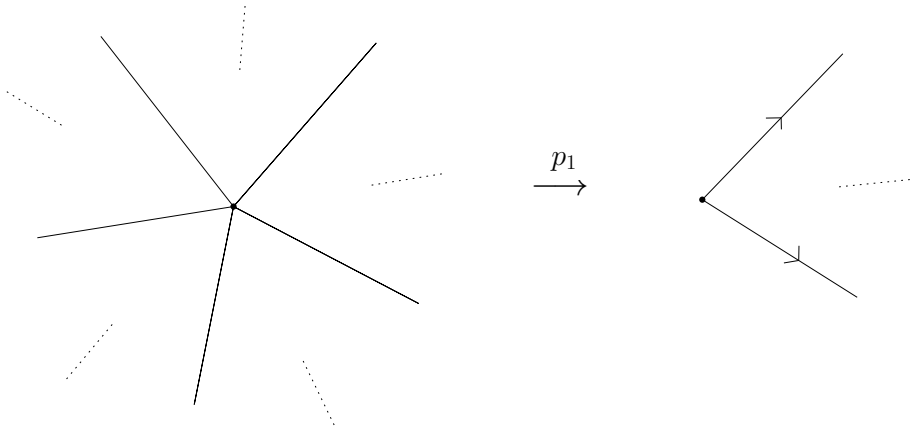

Figure 2.4: A planar section of a cyclic branched covering $p_1 : \mathbb{R}^3 \longrightarrow \mathbb{R}^3$ with 5 sheets. The dot in the middle of the covering set and of the base is the section of the line that constitues the branching set. On the right part the two half lines marked by arrows must be identified.

We want to show that, fixing the branching set as the trivial knot, choosing the order n of the branching set and requiring the covering set to be connected, the branched covering is unique and so it is as described above. Indeed, let us consider the complement $S^3 \setminus S^1$ of the branching set S^1. From the discussion above we can say that $\pi_1(S^3 \setminus S^1) \cong \pi_1(\mathbb{R}^3 \setminus l)$ and as $\mathbb{R}^3 \setminus l$ retracts on S^1 we have that $\pi_1(\mathbb{R}^3 \setminus l) \cong \mathbb{Z}$. As $\mathbb{Z}$ is abelian and cyclic all its subgroups are cyclic. Under this hypothesis we know that for any $n \in \mathbb{N}$ there exists just one subgroup $H \leq \mathbb{Z}$ with order n, hence the covering (which is completely determined by H) is also unique.

2.2.2 From knotoids to strongly invertible knots

Let us now proceed with the construction described above (following [1]). By the previous discussion, we can define the map $\gamma_S : \mathbb{K}(S^2) \longrightarrow \mathcal{K}(S^3)$ that associates to any knotoid $k \in \mathbb{K}(S^2)$ the preimage of the edge e_0 of its associated θ-curve $t(k)$ under the double branched covering $p : S^3 \longrightarrow S^3$ of S^3 branched along the preferred constituent unknot $e_- \cup e_+$. As the branching set is the trivial knot, by the previous remark the covering is unique and hence the map γ_S is well defined. Under this construction, any point of the edge e_0 of $t(k)$ (except to the endpoints v_0 and v_1) will have two different preimages, while the two endpoints, which belong to the branching set, will have just one preimage. Thus, we obtain an object that results to be homeomorphic to S^1, but that may be knotted in some way: in other words, a knot. An example can be seen in Figure 2.5.

Let us focus on the image $K = \gamma_S(k)$ of a knotoid $k \in \mathbb{K}(S^2)$. By construction, the group of the automorphisms of the covering p, which commutes with the fiber maps, has order 2. Thus, calling τ the non-trivial element of this group, it results that τ represents a non-trivial involution of the knot K. Hence, from the discussion made in Section 1.1, (K, τ) is a strongly invertible knot (for example, the Trefoil knot of Figure 2.5 is a strongly invertible knot). Since not every knot in S^3 is strongly invertible, the map γ_S is not surjective.

We are now ready to state and prove the main theorem of this section:

Theorem 2.3. *There is a 1-1 correspondence between unoriented knotoids, up to rotation, and knots K with a strong inversion τ, up to conjugacy.*

Proof. Recall some of the definitions of Chapter 1. $\mathcal{KSI}(S^3)$ is the set of strongly invertible knots (K, τ) in S^3 up to equivalence and $\mathcal{K}_{\mathcal{S.I.}}(S^3)$ is the subset of $\mathcal{K}(S^3)$ of knots that admit a strong inversion. There is then a natural forgetful map $\mathcal{KSI}(S^3) \longrightarrow \mathcal{K}_{\mathcal{S.I.}}(S^3)$.

Recall the map $\gamma_S : \mathbb{K}(S^2) \longrightarrow \mathcal{K}(S^3)$ defined above. As we saw, the lift of a knotoid through the double branched covering of S^3 is a strongly

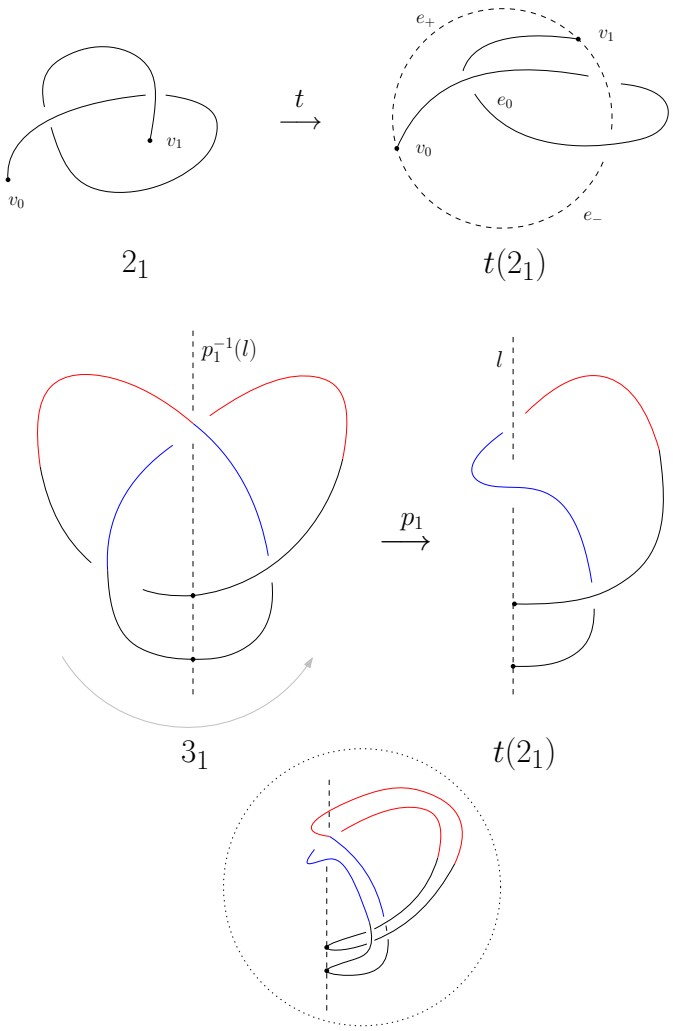

Figure 2.5: On the top: the knotoid 2_1 (see Appendix A) and its corresponding θ-curve $t(2_1)$. In the middle: the double branched cover p_1 from the Trefoil knot 3_1 (see Appendix A) to $t(2_1)$ (the preferred constituent unknot, now called l, is open as the figures are seen in $\mathbb{R}^3$). Same colours in the trefoil and in $t(2_1)$ indicate the parts that correspond to each other through the local homeomorphisms. The drawing inside the dotted circle at the bottom end of the figure represents a visual mid-step of the covering, that we hope it might help the reader. Moreover, the trefoil is a strongly invertible knot: $p_1^{-1}(l)$ constitues $\mathrm{Fix}(\tau)$, where τ is the involution given by the rotation of $\mathbb{R}^3$ around $p_1^{-1}(l)$ by angle π.

invertible knot, thus $\gamma_S(\mathbb{K}(S^2)) \subset \mathcal{K}_{\mathcal{SI}}(S^3)$. More precisely, the branching set $e_- \cup e_+$ determines an involution τ. Thus, we can promote γ_S to a map

$$\gamma_S : \mathbb{K}(S^2) \longrightarrow \mathcal{KSI}(S^3).$$

Furthermore, as two knotoids k and k_{rot} lift to θ-curves that differ by swapping the labels of the edges e_+ and e_- only, their double branched coverings produce isotopic knots, that is their images under the map γ_S are the same (recall Figure 2.3). The same is true for the knotoids k and $-k$. So, a knotoid k, its reverse $-k$, its rotation k_{rot} and its reverse rotation $-k_{\text{rot}}$ map to the same element in $\mathcal{KSI}(S^3)$. Hence, γ_S descends to a well defined map on the quotient

$$\gamma_S : \mathbb{K}(S^2)/_{\approx} \longrightarrow \mathcal{KSI}(S^3)$$

Let us now proceed in the opposite way. Let $(K, \tau) \in \mathcal{KSI}(S^3)$. Thanks to the positive resolution of the Smith conjecture (see [9]), the fixed point set of τ is an unknotted circle. Moreover, τ defines the projection

$$p : S^3 \longrightarrow S^3/\tau \cong S^3$$

that can be interpreted as the double covering of S^3 branched along $\text{Fix}(\tau)$, in the same way of the projection seen in Figure 2.5. So, from (K, τ) we can construct the θ-curve $\theta(K, \tau) = p(K) \cup p(\text{Fix}(\tau))$ where $p(K) = e_0$ and $p(\text{Fix}(\tau)) = e_- \cup e_+$. Equivalent strongly invertible knots project to equivalent θ-curves (seen as elements of $\Theta^s/_{\approx}$), thus, we have a well defined map

$$\beta : \mathcal{KSI}(S^3) \longrightarrow \Theta^s/_{\approx}.$$

The four labelled θ-curves corresponding to the different choices of labelling the edges e_-,e_0 and e_+ and the vertices v_0 and v_1 are mapped by the isomorphism t of Theorem 2.1 to knotoids k, $-k$, k_{rot} and $-k_{\text{rot}}$ related by reversion and rotation, as discussed above. So, given a strongly invertible knot there are four oriented knotoids associated to it. An example can be seen in Figure 2.6.

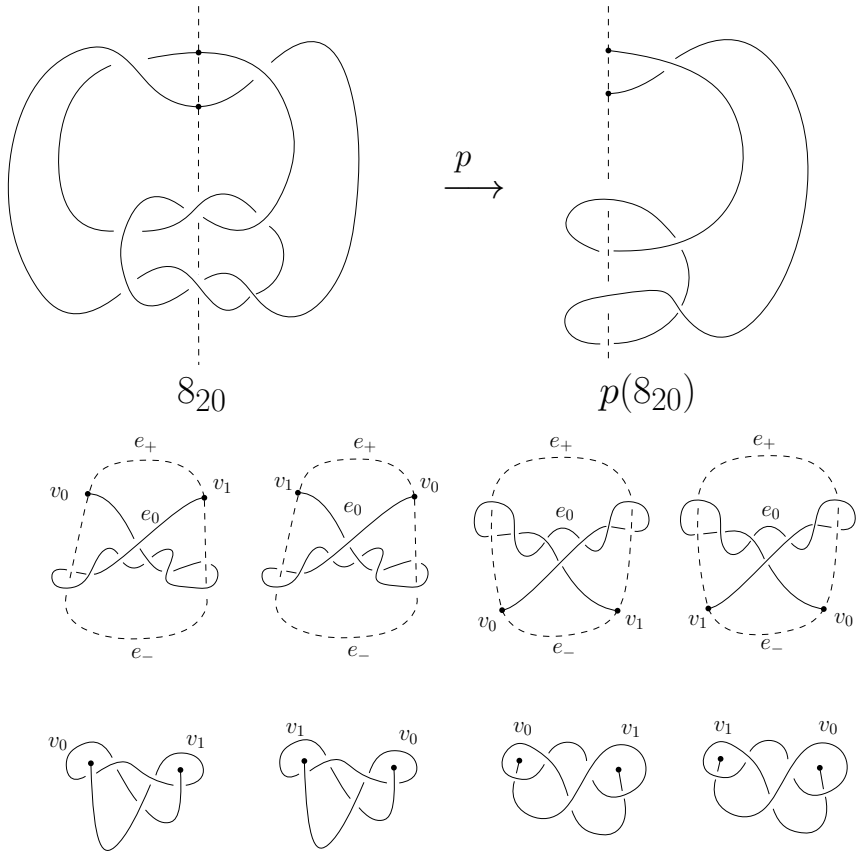

Figure 2.6: For example, the strongly invertible knot 8_{20} has 4 knotoids associated to it and as they represent the same knotoid up to rotation and reversion they belong to the same class in $\mathbb{K}(S^2)$. On the bottom there are the four θ-curves and the four knotoids associated to the projection of 8_{20}.

Thus, we have a well defined map

$$\Pi = t_{\approx}^{-1} \circ \beta$$

from the set of strongly invertible knots to the set of unoriented knotoids in S^2 up to rotation. Since the preferred constituent unknot of $t_{\approx}(t_{\approx}^{-1}(\theta(K,\tau)) = \theta(K,\tau)$ is clearly $p(\mathrm{Fix}(\tau))$, Π is the inverse of γ_S. From this and the discussion above we obtain that

$$\gamma_S : \mathbb{K}(S^2)/_{\approx} \longrightarrow \mathcal{KSI}(S^3)$$

is a bijection and hence the theorem is proved. □

2.3 Behaviour under forbidden moves

In this section we want to discuss, following [2], how forbidden moves behave under the constructions made in the previous sections of this chapter.

2.3.1 Forbidden moves and more

First, let us give a precise definition of forbidden move:

Definition 2.3. *Given a knotoid k, a **forbidden move** on the knotoid consists in pulling the strand adjacent to an endpoint over/under a transversal strand (recall Figure 1.3).*

Remark 3. Remember that performing a forbidden move on a knotoid diagram might result in changing the knotoid type. Moreover, any knotoid diagram can be transformed into the trivial one by a finite sequence of forbidden moves and vice-versa.

Given a knotoid k and its correspondent θ-curve $t_{\approx}(k)$, we will see that the result of a forbidden move on k is a strand passage (that is, a crossing change) on $t_{\approx}(k)$ between the arcs e_0 and either e_- or e_+. On the contrary, the consequences of the same forbidden move on the strongly invertible knot $\gamma_S(k)$ are a bit less straightforward:

Definition 2.4. *Let K_1 be a knot and let $b : I \times I \longrightarrow S^3$ be an embedding such that $K_1 \cap b(I \times I) = b(I \times \partial I)$. The knot $K_2 = (K_1 \setminus b(I \times \partial I)) \cup b(\partial I \times I)$ is said to be obtained from K_1 by a* ***band surgery*** *along the band $B = b(I \times I)$. If the knot is oriented, then a band surgery is called* ***coherent*** *if it respects the orientation of the knot K_1, otherwise it is called* ***non-coherent*** *(see Figure 2.7).*

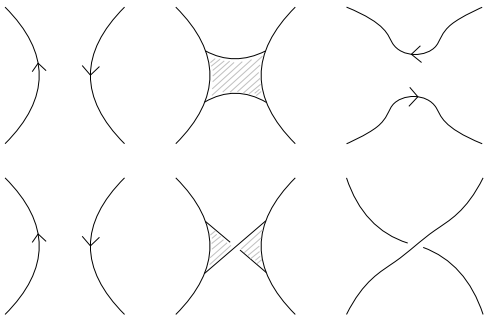

Figure 2.7: Local pictures of a coherent (top) and a non-coherent (bottom) band surgery.

A non-coherent band surgery transforms knots in knots (on the contrary, the result of a coherent band surgery may be a two components curve) and it is called a H_2**-move**. In particular, we will deal with

Definition 2.5. *Consider the strongly invertible knot (K_1, τ_1). We say that the strongly invertible knot (K_2, τ_2) is obtained from (K_1, τ_1) by an* ***equivariant band surgery*** *if K_1 and K_2 are related by a H_2-move such that*

- $\mathrm{Fix}(\tau_1)$ *intersects the band $b(I \times I)$ transversally exactly once in its interior and the band is invariant under τ_1;*
- (K_2, τ_2) *and (K_1', τ_1) are equivalent as strongly invertible knots, where K_1' is the knot obtained from K_1 by doing the band surgery.*

An example of equivariant band surgery is shown in Figure 2.8.

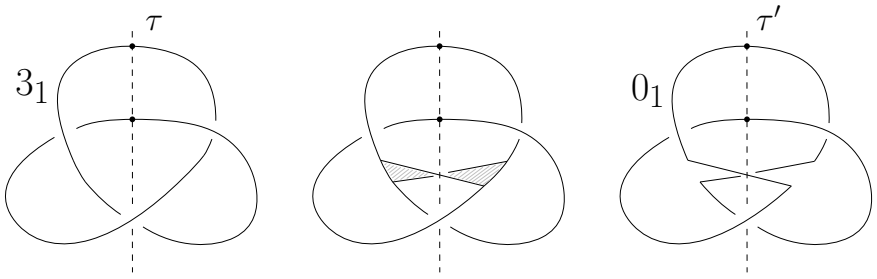

Figure 2.8: The strongly invertible knots $(3_1, \tau)$ and $(0_1, \tau')$ (see Appendix A) are related by an equivariant band surgery.

2.3.2 Equivalence under forbidden moves

We are now ready to state and prove the main result of this section.

Theorem 2.4. *Consider two equivalence classes of knotoids k_1 and k_2 up to reversion and rotation. Then the following are equivalent (see Figure 2.9):*

1. *k_1 and k_2 differ by a single forbidden move;*
2. *their corresponding θ-curves $t_{\approx}(k_1)$ and $t_{\approx}(k_2)$ differ by a single strand passage between the edge e_0 and either e_- or e_+;*
3. *their corresponding strongly invertible knots $\gamma_S(k_1)$ and $\gamma_S(k_2)$ differ by an equivariant band surgery.*

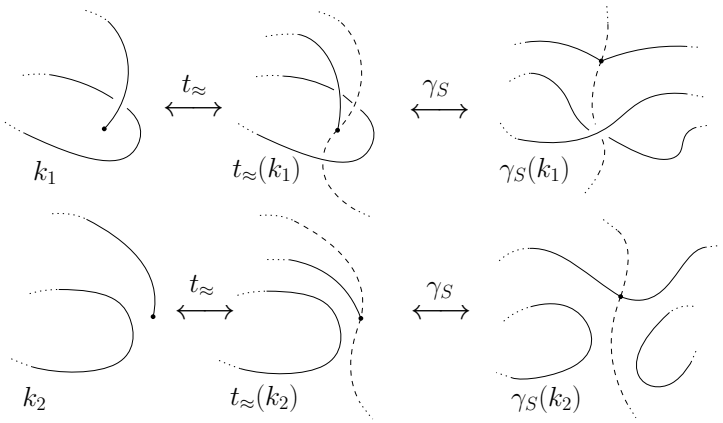

Figure 2.9: A forbidden move between two knotoids k_1 and k_2 (on the left) induces a strand passage between the arcs e_0 and $e_\pm$ between the corresponding θ-curves (in the middle) and an equivariant band attachment between the corresponding strongly invertible knots (on the right).

Proof. ($3 \Rightarrow 2$) Consider an equivariant band surgery between two strongly invertible knots (K_1, τ_1) and (K_2, τ_2). Up to ambient isotopies fixing the circle $\mathrm{Fix}(\tau)$ the band attachment locally looks like the one in the top part of Figure 2.10, with possibly the opposite twists on the band. On the quotient $S^3/\tau_1 \cong S^3$ this results in a strand passage between the arcs e_0 and one between e_- and e_+ in the θ-curve $p(\mathrm{Fix}(\tau_1)) \cup p(K)$, as shown in the bottom of Figure 2.10.

($2 \Rightarrow 1$) Consider then a simple θ-curve. Up to ambient isotopies fixing the circle $e_- \cup e_+$, any strand passage between the arc e_0 and the arc $e_\pm$ locally looks like the one in the top part of Figure 2.11 (up to changing the crossing between e_0 and $e_\pm$). The bottom right part of Figure 2.11 shows how this translates into a forbidden move on the corresponding knotoid. The case where the crossing between e_0 and $e_\pm$ is the opposite one is similar.

($1 \Rightarrow 3$) The procedure is analogous as above. Consider two generic knotoids that differ by a forbidden move. Up to isotopies and Reidemeister moves they can be depicted as in bottom part of Figure 2.12. Then, their correponding strongly invertible knots given by the map γ_S and depicted on top part of Figure 2.12 differ by an equivariant band attachment (as you can

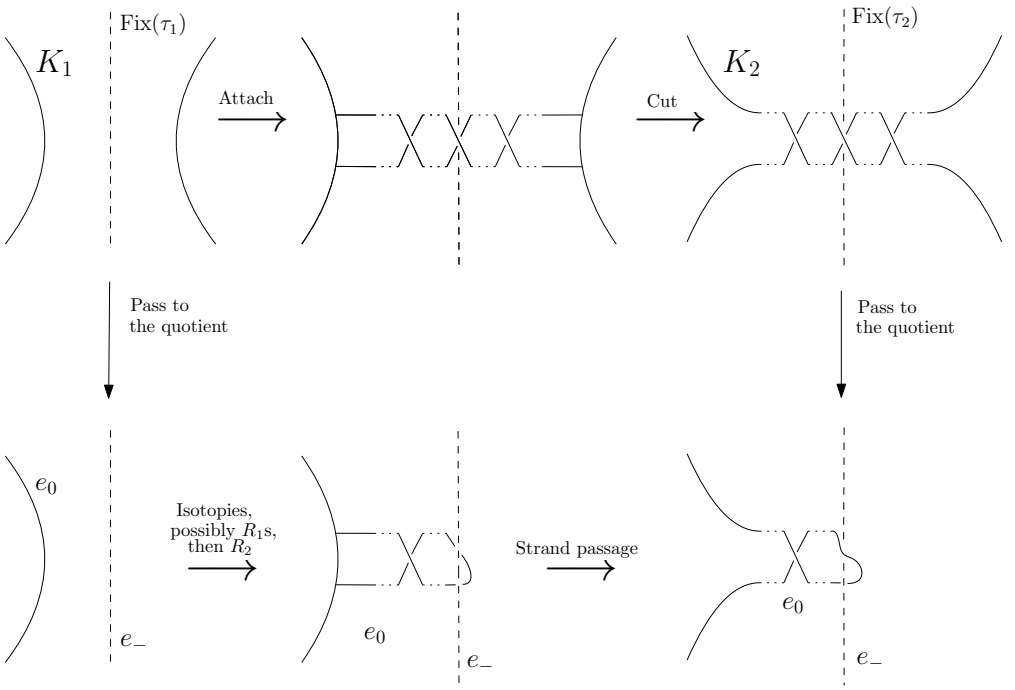

Figure 2.10: On the top, two strongly invertible knots (K_1, τ_1) and (K_2, τ_2) related by an equivariant band attachment. Up to isotopies fixing the circle Fix(τ) (and up inverting the crossings) the band looks like the one in the middle of the top row. By Definition 2.5 the band has an odd number of twists. On the bottom, the corresponding effect on the associated θ-curves. If the band has $2n+1$ twists, the θ-curves are related by a sequence of n Reidemeister moves Ω_1 followed by one Reidemeister move Ω_2 and by a single strand passage.

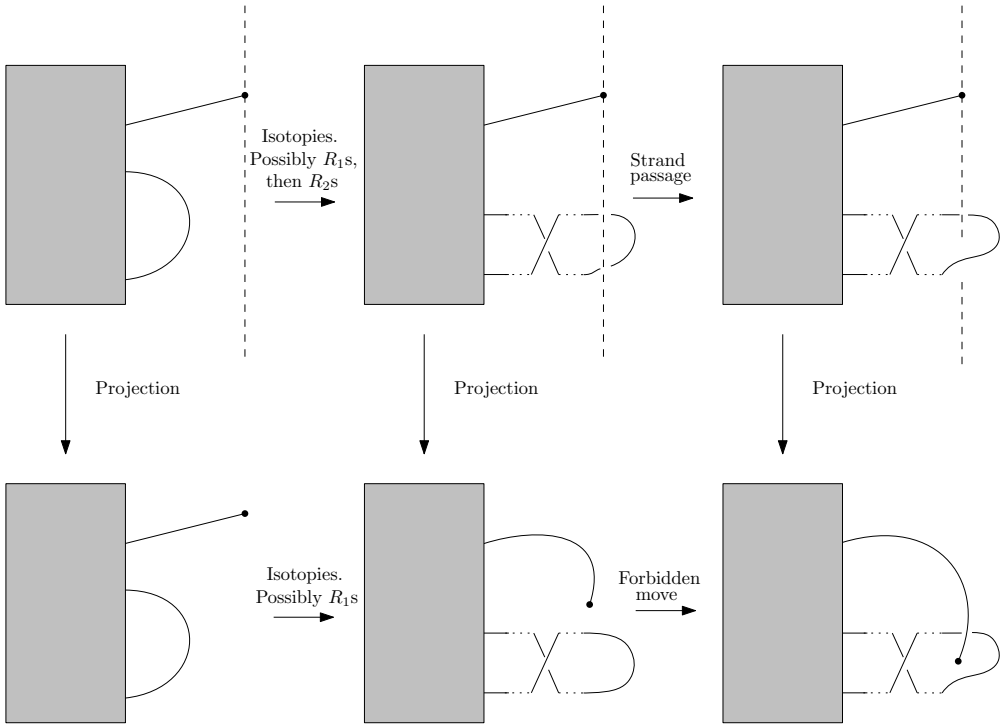

Figure 2.11: On the top row, two θ-curves related by a strand passage between the arc e_0 and the arc $e_\pm$. Up to ambient isotopes preserving the circle $e_- \cup e_+$ we can make the strand passage look like in the picture. The effect on the corresponding projections giving the knotoids on the bottom row is to perform a sequence of Reidemeister moves Ω_1 followed by a single forbidden move.

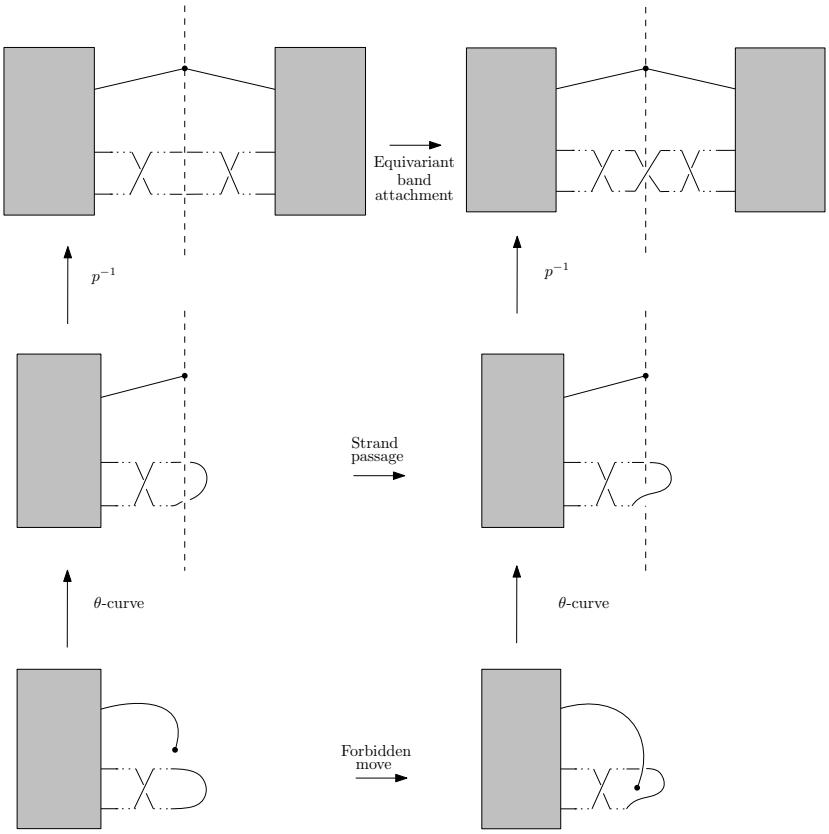

Figure 2.12: On the bottom row, two knotoids that differ by a forbidden move. The corresponding θ-curves (in the middle row) and strongly invertible knots (in the top row) are obtained using the construction explained in Sections 2.1 and 2.2. The strongly invertible knots differ by an equivariant band attachment.

see from the figure). The case of the other type of forbidden move is similar to the one described in Figure 2.12.

□

2.4 f-distance and its computation

In this section we analyse the relation between any two knotoids in terms of forbidden moves (following [2]). In particular, we explain how to define a forbidden moves-based distance and we discuss a method to numerically

compute a table of the distances between any two knotoids with minimal crossing number less or equal to four.

Recall Definition 2.3 and Remark 3. Thus, we can define a forbidden move-based distance for knotoids:

Definition 2.6. *Given two knotoids k_1 and k_2, their* ***forbidden move-distance****, or f-distance $d_f(k_1, k_2)$, is the least number of forbidden moves across all the representatives of k_1 and k_2 needed to transform k_1 into k_2.*

Recall then Definition 2.5. Even in this case we can define a distance between strongly invertible knots, that bases on the number of equivariant band surgeries that relates the two strongly invertible knots:

Definition 2.7. *Given two knots K and K' their* ***H_2-Gordian distance*** *$d_{H_2}(K, K')$ is the minimal number of equivariant band attachments connecting K and K' (among all the elements of their equivalence classes).*

From now on we will use the word "knotoids" to indicate any equivalence class of elements of $\mathbb{K}(S^2)$ up to the four involutions of Figure 1.5. As a direct consequence of this new definition and of Theorem 2.4 we have that given two knotoids k_1 and k_2 and their associated strongly invertible knots $\gamma_S(k_1) = (K_1, \tau_1)$ and $\gamma_S(k_2) = (K_2, \tau_2)$ it holds that

$$d_f(k_1, k_2) \geq d_{H_2}(K_1, K_2). \tag{2.1}$$

Analogously, for any knotoid k let us call $K_k^{\pm}$ the constituent knots of $t_{\approx}(k)$ given by $e_0 \cup e_{\pm}$ respectively. We can define

Definition 2.8. *Given two knotoids k_1 and k_2, consider the pairs $(K_{k_1}^+, K_{k_1}^-)$ and $(K_{k_2}^+, K_{k_2}^-)$. Their* ***Gordian distance*** *d_{pair} is defined as*

$$\begin{aligned} d_{\text{pair}}((K_{k_1}^+, K_{k_1}^-), (K_{k_2}^+, K_{k_2}^-)) = \min\{&d_{H_2}(K_{k_1}^+, K_{k_2}^+) + d_{H_2}(K_{k_1}^-, K_{k_2}^-), \\ &d_{H_2}(K_{k_1}^+, K_{k_2}^-) + d_{H_2}(K_{k_1}^-, K_{k_2}^+)\}. \end{aligned}$$

Consider the equivalent facts (1) and (2) of Theorem 2.4. It is clear that any strand passage that relates two θ-curves must affect either $K_{k_1}^+$ or $K_{k_1}^-$

and it cannot change both these constituent knots simultaneously. From this and from the new definition of knotoids it follows that

$$d_f(k_1, k_2) \geq d_{\text{pair}}((K^+_{k_1}, K^-_{k_1}), (K^+_{k_2}, K^-_{k_2})) \tag{2.2}$$

In [2] the authors compute a table of the f-distances of knotoids with up to four crossings, proceeding in the following way. Consider all the knotoid diagrams with up to 4 crossings (counting both those of minimal and non-minimal crossing number representation). Identify the knotoids using some knotoid invariants. The lower bounds for the f-distances for any pair of knotoids are found with the help of equations 2.1 and 2.2 and using results of knot theory. We then have to produce the upper bounds. Call $\mathcal{K}$ the set of all knotoid diagrams with up to four crossings, we can build an undirected graph $G(V, E)$ with set of vertices V and set of edges E such that

$$V(G) = \mathcal{K}$$
$$E(G) = \{(v, u) \mid (v, u) \in \mathcal{K}^2, v \neq u, v \sim_f u\}$$

where $v \sim_f u$ denotes a pair of knotoid diagrams (v, u) that are related by a single forbidden move. Thus, G is the undirected graph where the vertices are all the knotoids with up to four crossings and the edges connect knotoids that are related by a single forbidden move. G was numerically computed by the authors, and with it the path that minimises the number of forbidden moves between any pair of vertices. Once the set of diagrams is partitioned into isotopy classes, the path of minimal distance between any two isotopy classes determines their numerical f-distance d_f^{num}. Thus, it was possible to obtain an upper bound between isotopy classes of knotoids by computing their **experimental f-distances** defined as

$$d_f^{\text{exp}}(v, u) = \min\{d_f^{num}(v, x) \mid x \in (u, u_m, \text{sym}(u), u_{\text{rot}})\}.$$

The comparison of the lower bounds with the upper bounds leads to the table of Figure 2.13.

	0_1	2_1	3_1	3_2	4_1	4_2	4_3	4_4	4_5	4_6	4_7	4_8
0_1	0	1	2	1	2	1	2	2	2	3	1	1
2_1	1	0	1	2	3	1	1	1	1	2	1	1
3_1	2	1	0	3	4	2	2	1	2	1	2	2
3_2	1	2	3	0	1	2	2-3	3	1	3-4	2	2
4_1	2	3	4	1	0	3	3-4	4	2	4-5	3	3
4_2	1	1	2	2	3	0	1-2	1	2	2	1-2	1
4_3	2	1	2	2-3	3-4	1-2	0	2	2	1	1-2	1
4_4	2	1	1	3	4	1	2	0	2	1	1-2	1
4_5	2	1	2	1	2	2	2	2	0	2-3	1-2	2
4_6	3	2	1	3-4	4-5	2	1	1	2-3	0	2-3	2
4_7	1	1	2	2	3	1-2	1-2	1-2	1-2	2-3	0	1-2
4_8	1	1	2	2	3	1	1	1	2	2	1-2	0

Figure 2.13: The f-distance table for equivalence classes of knotoids with minimal crossing number ≤ 4, taken from [2]. In a few cases (e.g. for the pair $(4_1, 4_6)$)) lower and upper bounds do not coincide. In these cases the table shows the extremes of the range of the possible values, separated by a dash. The colour blue marks the cases in which the lower bounds were found using inequality 2.2, while the red colour marks the cases in which inequality 2.1 was used. The authors were not able to produce lower bounds for the entries in orange.

Chapter 3

Applications

In this chapter we see some of the applications that the theory developed so far can have. In particular we deal with the modellisation of proteins, application that has recently become of great interest. In Section 3.1 we analyse how a protein can be studied, using the diagram of the projections of its associated knotoids. In Section 3.2 we find a numerical measure for recognising deeply knotted proteins, which is fairly useful in detecting the enzymatic state of the protein. We will follow [2].

3.1 Knotoids as protein projections

Proteins are long linear biomolecules that often fold into conformations with non-trivial topology. By tracing the coordinates of their essential contituents, that is the carbon atoms that are contained in the amino acids that form the protein (also called Cα atoms), one can model them as open polygonal curves in the 3-space. Analysing the knottedness of a proten can be extremely useful in determining some of its main features (we see it in Section 3.2) and knotoids are a good tool for doing this.

The general idea behind the use of knotoids is to characterise the **global topology** of each protein chain (that is, the topology of the whole chain) by assigning a knotoid type to it. The authors of [2] considered the modelled

protein as inside a large enough sphere centered at the center of mass of the chain. In this way, choosing a point on the surrounding sphere determines a planar projection of the protein: they considered the plane tangent to the sphere orthogonal to the direction highlighted by the center of the sphere and the chosen point. The result is a knotoid diagram. Note that different planes of projection may yield different knotoid diagrams, hence determining the knotoid type of a protein using a single projection is far from being accurate (see Figure 3.1).

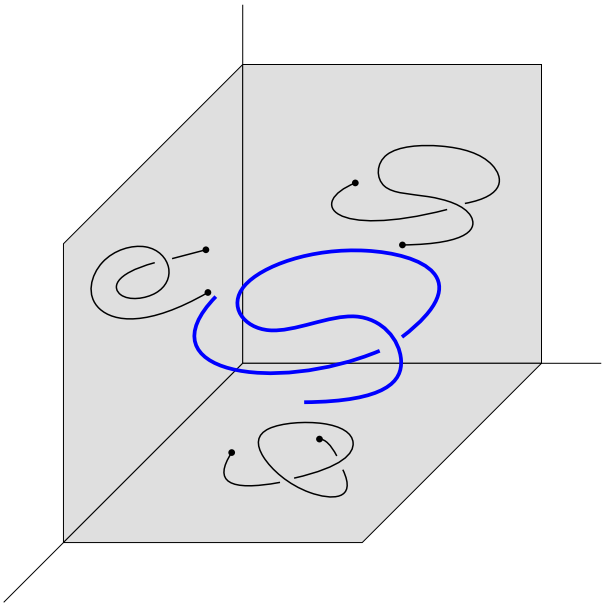

Figure 3.1: An example of how different planes of projection for the same protein may lead to different knotoids.

In principle, it is possible to consider the knottedness of any open ended-curve in the 3-space as a distribution (also called spectrum) of knotoid types corresponding to the knotoid diagrams resulting from the projections described above. The knotoid with the highest probability in the distribution of knotoid types over all projections characterises the protein and it is called the **predominate knotoid**. In order to obtain an unbiased overview of a protein topology the authors would have to consider all possible projections. However, since this is not computationally feasible, the distribution

was approximated by sampling from the space of all possible projections.

To this end, they wanted to determine the knotoid types of all the projections considered. To simplify this process, for any projection the knotoid type was maintained under ambient isotopies by the introduction of two lines orthogonal to the projection plane and that passes through the endpoints of the diagram (they are similar to the lines introduced in Figure 2.1). Moreover, an algorithm to simplify, but at the same time to preserve the underlying topology of the protein, was applied. Eventually, the knotoid types were determined using knotoid invariants.

The above data was summarised in a plot called the **projection map** of the protein. This diagram can be computed using the following concepts (see [5]). Given a finite set of points S in the euclidean space $\mathbb{R}^n$ the **Voronoi cell** of a point $s \in S$ is defined as $V_s = \{x \in \mathbb{R}^n \mid\mid\| x - s \|\leq\| x - v \|, v \in S\}$, that is, the set of points for which s is the closest among the points of S. Note that V_s is a convex polyhedron in $\mathbb{R}^n$, that any two Voronoi cells meet at most in a common piece of their boundary and together the Voronoi cells cover the entire space. The **Voronoi diagram** $\mathcal{VD}$ of the set S is the collection of Voronoi cells of its points (see Figure 3.2). In the authors' case the plot consists in the Voronoi diagram of S^2 with respect to the set of points sampled from S^2. Furthermore, they coloured each cell of the projection map according to the knotoid type it produces. By construction, there is a bijection between the number of different colours in the projection map and the number of different knotoids in the spectrum of the analysed curve. An example can be seen in Figure 3.3.

Both the spectrum and the projection map depend heavily on the sample size of projections; if too few points are sampled, then the overall topology of the analysed curve will not be well approximated. The authors studied this aspect in depth, in order to numerically approximate the optimal size of the sample set of projections. The procedure worked as follows. They considered a generic projection of a protein chain on some plane and called k the corresponding knotoid. If they continuously perturbed the projection direction

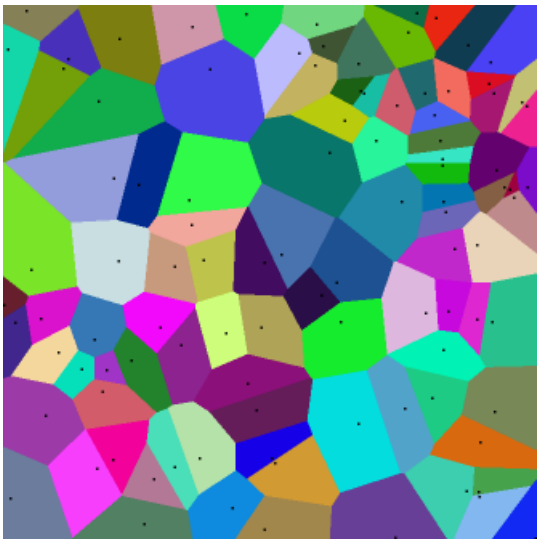

Figure 3.2: A Voronoi diagram of $\mathbb{R}^2$ given by the minimisation of the distances from a finite set of points $S \subset \mathbb{R}^2$ (in black). Points associated to the same $s \in S$ are coloured in the same way. This figure is taken from https://it.wikipedia.org/wiki/Diagramma_di_ Voronoi.

until the knotoid type changed to k', they obtained a pair of knotoids with $d_f(k, k') > 0$. Using a smaller sample set led to a triangulation of S^2 that produced a Voronoi diagram with wider cells. Therefore, there was a higher chance for cells corresponding to knotoids with $d_f > 1$ to be adjacent. Since the predominate knotoid corresponds to the largest region of the projection map, they argued that it was sufficient to focus on the the discrepancies between the region of the predominate and its immediate neighbours. For this, they defined the following concepts:

Definition 3.1. *The* ***interface error*** $\mathrm{er}(s)$ *associated to a sample set of size* s *of a projection map defined as above is the ratio of the number of regions - adjacent to the region of the predominate knotoid* k_0 *- that correspond to knotoids* k_i *for which* $d_f(k_0, k_i) > 1$ *over the number of all adjacent regions to* k_0*.*

Definition 3.2. *The* ***spectrum*** $\mathrm{Spec}(s)$ *of a projection map defined as above is the number of distinct knotoids in the approximated knotoid distribution*

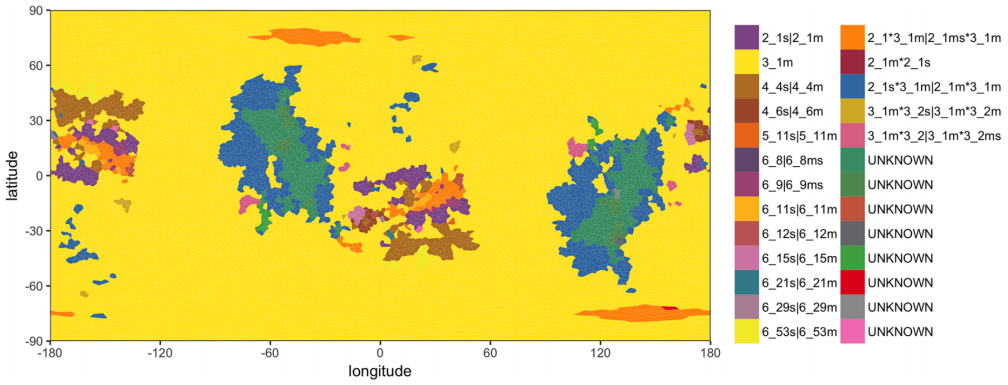

Figure 3.3: The projection map for the protein N-acetyl-Lornithine transcarbamylase complexed with N-acetyl-Lornirthine. This map (that is taken from [2]) is made using 10,000 projections. The predominate knotoid is 3_1^m as it corresponds to the region with the biggest area. In the legend, the symbol "|" stay for "or" while the label "UNKNOWN" corresponds to knotoids with minimal crossing number greater than six.

obtained considering s randomic projections.

The authors wanted to see how these two coefficients were related to each other. In particular, they analised all the proteins with predominate knotoid type 3_1 (see Appendix A) multiple times, using an increasing number of random projections: 50, 100, 500, 1,000, 5,000 and 10,000 projections. Each time er(s) and Spec(s) for the respective Voronoi diagram were calculated. Computing the Spearman correlation coefficient[1] r between er(s) and Spec(s), they noticed that increasing the number of projections the correlation between the two coefficient became lower. In other words, at 10,000 projections they had the most accurate overview of the topology of the protein. It is interesting to see that this fact agrees with the idea that increasing the number of projections the Voronoi cells become smaller, and so the possibility of having pairs of adjacent cells with $d_f > 1$ becomes weaker.

We conclude this section reporting another aspect found out by the authors: the differences between the results obtained using 5,000 and 10,000

[1]See https://en.wikipedia.org/wiki/Spearman%27s_rank_correlation_coefficient

projections respectively were not significant, so analysing a protein with 5,000 projections may provide the best compromise between computational speed and accuracy.

3.2 Deeply knotted proteins

In this section we analyse the concept of "knottedness" associated to a protein and we give a numerical estimate for determining whether a protein is deeply knotted or not (following [2]).

Knotted proteins are proteins whose backbones entangle themselves in a knot (pulling from both termini). Let us give a more precise definition. As in Section 3.1, for a given protein consider the associated polygonal curve determined by its Cα atoms and a large enough sphere centered at the center of mass of the chain. Choose then some randomic points on the sphere. For any point p chosen in this way, connect it to the termini of the protein with two segments that do not meet with the polygonal curve, exept for the endpoints: we hence obtain a knot. Identifying the knot and repeating this procedure for any chosen p we obtain a distribution of knots associated to the protein. If the knot-type that characterises the protein (the one that has the highest probability in the distribution of the associated knots) is not the trivial knot 0_1 (see Appendix A) we say that the protein is **knotted**. In a knotted protein we call **knotted core** its shortest subchain that closed **as above** forms a knot; the subchains located before and after the knotted core are called the **N-tail** and the **C-tail**, where N and C are the two termini of the protein, as in Figure 3.4. A knotted protein, that can be seen as an open polygonal knot in the 3-space, is considered **deep** if several vertices from either side of the knotted core have to be removed before making the knot trivial. Thus, the depth of a protein relates to the ability of the protein to resist unknotting (removing residues from both sides).

Determining whether a protein is deeply knotted or not can be extremely useful. Indeed, the vast majority of proteins are enzymes where there is an

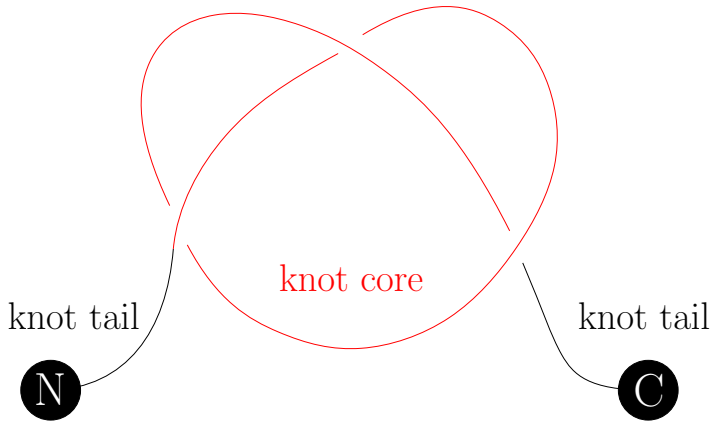

Figure 3.4: The core (in red) and the tails (in black) of an open knot representing a protein with a trefoil knot. The two beads on either side represent the two termini, N and C respectively, of the protein chain.

overlap between knotted cores and the respective enzymatic sites. Furthermore, these sites are either located inside or close to the knotted core of the chain. In this context, it was shown that knotted cores play a vital role in some aspects of a protein structure and function. Moreover, it was observed that the formation of deep knots with characteristic structural motifs provides a favourable environment for active sites in enzymes.

One strategy that can be used to detect these local knots is the subchain analysis. With this method all possible subchains of the protein are analysed and this is computationally achieved by progressively trimming the chain from each side and evaluating its knotoid type until the knotted core is obtained. Basing on this technique, we can define an abstract measure of depth, denoted by $D(k)$, as follows:

$$D(k) = \frac{l_N(k) l_C(k)}{l_T^2(k)}$$

where k is a knotoid, $l_T(k)$ is the total lenght of the chain of k, $l_N(k)$ is the lenght of the N-tail of k and $l_C(k)$ is the lenght of the C-tail of k.

As the subchain analysis depends on the total lenght of the protein, it can be computationally heavy. Thus, the authors of [2] thought that it would be useful if the tightness of a knot could be numerically determined from

the global topology analysis. For this purpose they introduced a numerical measure, the relative area, defined in the following way. First, let us give two preliminary definitions:

Definition 3.3. *Let k be a knotoid in S^2. An **interface knotoid**, denoted by k_{int}, is a knotoid such that:*

$$d_f(k, k_{\text{int}}) = 1 \quad \text{and} \quad d_f(k_{\text{int}}, 0_1) \leq 1$$

where 0_1 is the trivial knotoid (see Appendix A).

Definition 3.4. *The **relative area** $\mathcal{A}_{\text{rel}}$ is the ratio of the sum of the areas of interface knotoids in the $\mathcal{VD}$ over the area of the predominate, namely:*

$$\mathcal{A}_{\text{rel}} = \frac{1}{\mathcal{A}_p} \sum_{k \in \mathcal{K}_{\text{int}}} \mathcal{A}_k \tag{3.1}$$

where $\mathcal{K}_{\text{int}}$ is the set of all interface knotoids of the predominate knotoid, $\mathcal{A}_p$ is the area in the $\mathcal{VD}$ of the predominate knotoid and $\mathcal{A}_k$ is the area in the $\mathcal{VD}$ of the knotoid k.

Usually, a deep protein is also tightly knotted as the length of its knotted core is relatively small, compared to the knot overall length. The idea behind the strategy proposed in [2] is assuming that the deeper a knot is, the smaller the total area of the interface knotoids will be in the $\mathcal{VD}$. This is because the two tails of the knot are less probable to interact with the rest of the chain in a way that will produce a forbidden move. Since the knot is deep, it will also be relatively tight, hence the regions of the corresponding diagram will be smaller. Thus, the probability of having large areas in the $\mathcal{VD}$ corresponding to interface knotoids will be smaller. The authors made some experiments to evaluate the relation between $\mathcal{A}_{\text{rel}}$ and $D(k)$. They analysed all proteins that form a 3_1 knot (see Appendix A). From Theorem 2.4 the knotoid 2_1 (see Appendix A) is the only knotoid with f-distance 1 from both 0_1 and 3_1 (it can be seen checking that any other knotoid with f-distance 1 from 3_1 has distance >1 from 0_1 using inequality 2.2). In this case equation 3.1 became:

$$\mathcal{A}_{\text{rel}} = \frac{\mathcal{A}_{2_1}}{\mathcal{A}_{3_1}}$$

They then computed $\mathcal{A}_{\text{rel}}$ and $D(k)$ for all the 457 studied proteins, computing the $\mathcal{VD}$ using the optimal value of 5,000 projections found in Section 3.1. The strong decreasing monotonous relation between the two coefficients given by their Spearman coefficient allowed them to conclude that the value $\mathcal{A}_{\text{rel}} = 0.2$ represents the boundary for detecting deeply knotted proteins from shallow ones: values $\mathcal{A}_{\text{rel}} \leq 0.2$ are likely to correspond to a protein having a deeply knotted trefoil, while values $\mathcal{A}_{\text{rel}} > 0.2$ usually refer to shallow proteins. There are some outliers of this two clusters, but it does not seem that there is any relevant correlation between them.

To conclude, this new quantity $\mathcal{A}_{\text{rel}}$ seems to be a good coefficient to determine whether a protein is deeply knotted or not.

Appendix A

This appendix includes two tables.

The first one is the table of all distinct knotoids in the sphere S^2 with minimal number of crossings of a knotoid diagram up to four crossings . These knotoids have been distinguished by the use of some knotoids invariants. The notation follows the one in [4], that uses the scheme X_Y, where X is the minimal number of crossings of the knotoid and Y is the relative position among all knotoids with the same number of crossings.

The second one is the table of all distinct prime knots with minimal number of crossings up to eight crossings taken from [7]. These knots have been distinguished by the use of a well known knots invariant called the Alexander polynomial. In particular, the notation is similar to the one used for knotoids and it takes the name of Alexander-Briggs notation (see [7]).

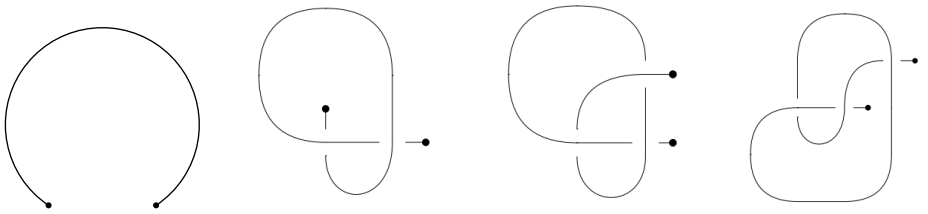

(a) 0_1 (b) 2_1 (c) 3_1 (d) 3_2

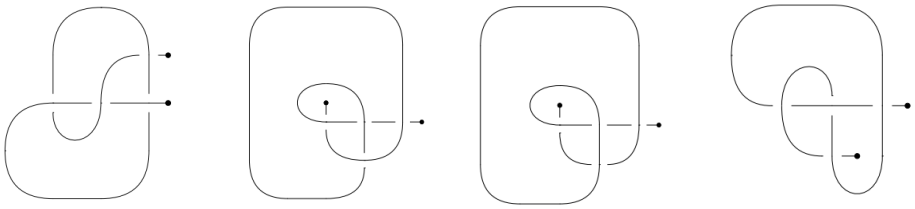

(e) 4_1 (f) 4_2 (g) 4_3 (h) 4_4

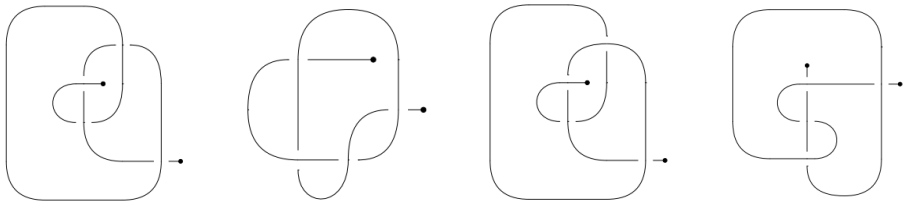

(i) 4_5 (j) 4_6 (k) 4_7 (l) 4_8

Figure A.1: Table of knotoids with up to four crossings. The pictures (exept for the trivial knotoid 0_1) are taken from [4].

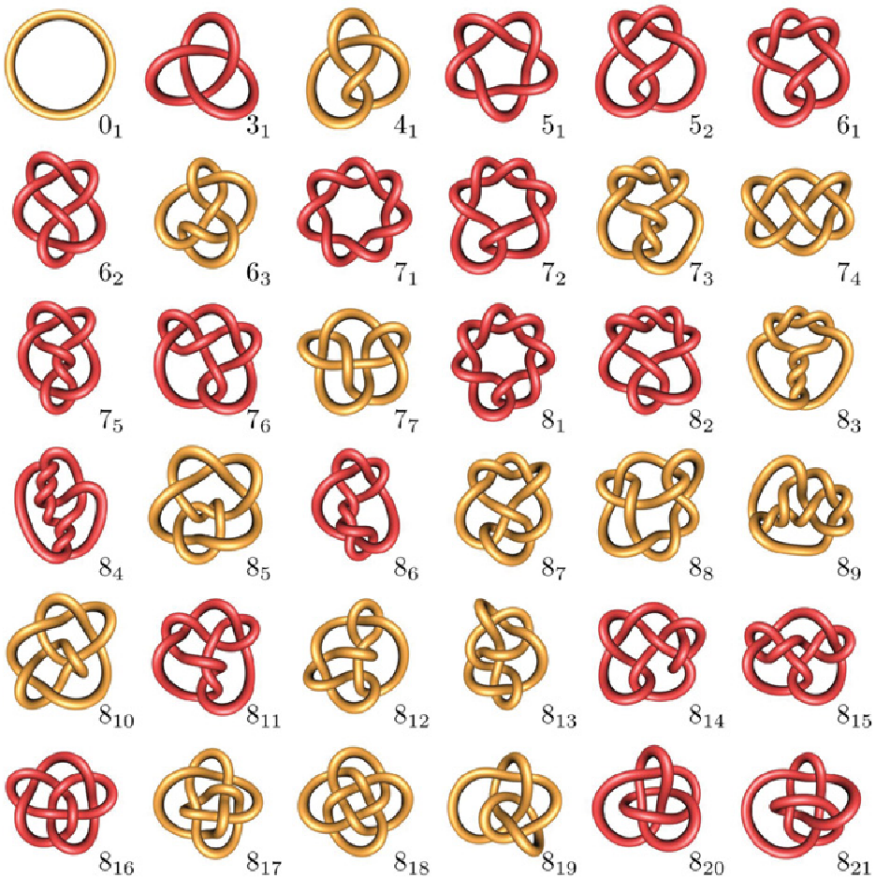

Figure A.2: Table of knots with minimal number of crossings up to 8 crossings. This figure is taken from https://www.semanticscholar.org/paper/New-biologically-motivated-knot-table.-Brasher-Scharein/aac22f9e6d967d83991c5797f90fae26525ccd53.

Bibliography

[1] H. A. Harrington A. Barbensi D. Buck and M. Lackenby. "Double Branched Covers of Knotoids". In: *Comm. Anal. Geom* (2018). To appear, arXiv:1811.09121.

[2] A. Barbensi and D. Goundaroulis. "f-distance of Knotoids and Proteine Structure". arXiv:1909.08556. 2019.

[3] G. Burde and H. Zieschang. *Knots*. Walter de Gruyter, 2003.

[4] J. Dorier D. Goundaroulis and A. Stasiak. "A systematic classification of knotoids on the plane and on the sphere". arXiv:1902.07277v2. 2019.

[5] H. Edelsbrunner and J. L. Harer. *Computational topology, an introduction*. American Mathematical Society, Providence, RI, 2010.

[6] V. V. Prasolov and A. B. Sossinsky. *Knots, Links, Braids and 3-Manifolds*. American Mathematical Society, Providence, RI, 1997.

[7] D. Rolfsen. *Knots and Links*. American Mathematical Society, Providence, RI, 2003.

[8] V. Turaev. "Knotoids". In: *Osaka J. Math.* 49 (2012), pp. 136, 137.

[9] F. Waldhausen. "Uber Involutionen der 3-Sphare". In: *Topology* 8 (1969), pp. 81–91.